Failure Performance of Synthetic Fibre-Reinforced Warm-Mix Asphalt

Christian Gerald Daniel

FAILURE PERFORMANCE OF SYNTHETIC FIBRE-REINFORCED WARM-MIX ASPHALT

MSc THESIS

CHRISTIAN GERALD DANIEL

2018, Delft

FAILURE PERFORMANCE OF SYNTHETIC FIBRE-REINFORCED WARM-MIX ASPHALT

THESIS

for the degree Master of Science (MSc) in Structural Engineering,
Faculty Civil Engineering, Delft University of Technology

by

CHRISTIAN GERALD DANIEL

born in Makassar, Indonesia

Graduation Committee:

Prof. Dr. Sandra Erkens (TU Delft)

Dr. Xueyan Liu (TU Delft)

ir. Panos Apostolidis (TU Delft)

ir. Lambert Houben (TU Delft)

Dr. Yuguang Yang (TU Delft)

Henk Hilverink (Dutch Fiber Trading B.V.)

Mahesh Moenielal (DIBEC)

Ronald Diele (Schagen Infra B.V.)

Acknowledgements

This master thesis project has been conducted since last year with the purpose to achieve Master of Science in Civil Engineering at Delft University of Technology, Delft, The Netherlands. The project itself was made possible through the collaboration between the Pavement Engineering section of TU Delft and the provision of material from DIBEC as well as Dutch Fibre Trading. Many persons have been involved in supporting this project, whom I would love to thank for.

First and foremost, my most gratitude to Jesus Christ for everything He has done through the entire moment of my life, in particular when doing this thesis work. Without His grace and mercy, I would not have been able to perform well and tackle every issue that I have encountered.

A huge and sincere thanks to my thesis committee. Especially to Dr Xueyan Liu as my supervisor, as the first person who gave me a possibility for doing this thesis project. I would love to appreciate his availability for having discussion and giving suggestions during the project, as well as his professional attitude that has kept me motivated when doing this research. Another huge appreciation to ir. Panos Apostolidis, who has given numerous critical suggestions and spared his time to help me to overcome any challenge during this thesis work, as well as giving insights in each discussion; wish you success in your career and personal life. Also for the other supervisors such as Prof Sandra Erkens, ir. Lambert Houben, Dr Yuguang Yang, Henk Hilverink, Mahesh Moenielal, and Ronald Diele for their availability to become the part of the committee.

Other parties who have had a massive role during this thesis work are the guys from the laboratory. The Pavement Engineering lab crews (Marco Poot and Michele van Aggelen) who have provided a massive effort of assistance and giving valuable input so that each examination. Also to Paul Vermeulen from DEMO, who has put an enormous amount of help over the pull-out test as well as his kindness to give access to use several pieces of equipment.

Last but not least, a big hug and love to my parents and little sister, who has been steadily in giving me mental and physical support during my three years of study in The Netherlands with their unending love and prayers. Also to the beloved Mazmuria Irene Imanuella, who has always shown her love and care, and she has never failed to cheer me up.

To conclude, I strongly hope that this research project could serve a significant contribution to the progression of the pavement engineering field.

Summary

The use of synthetic fibres has been reported to enhance the performance of asphalt pavement materials in terms of permanent deformation, fatigue and thermal cracking. However, limited results about the benefits of synthetic fibres in the reinforced warm-mix asphaltic materials, and the exact mechanism of reinforcing the binding part in pavement structures is still unclear. This research aims firstly to examine the material at the warm mixed mortar level using a combination of two synthetic fibres (aramid and polyolefin) to conclude its fracture performance. Several laboratory tests were performed using specially designed experimental tools. Samples of three different fibre contents (0.05%, 0.1% and 0.5% of specimen weight) and two fibre lengths (19 and 38mm) were evaluated. In particular, pull-out tests, whose objective was to explore the interaction of fibre-matrix demonstrated a matrix-type of fracture; meaning that the adhesion of fibre-matrix is higher than the strength of the matrix itself, which implies a benefit of adding fibre to a mixture at high service temperature.

Moreover, direct tension tests were carried out with both monotonic and cyclic loading to measure the effect of the synthetic fibres on tensile strength, fracture energy and fatigue life of reinforced warm mixes under monotonic and cyclic tension load, respectively. These tension experiments concluded improvements on mechanical characteristics of warm mixed asphalt mortars when fibres were added, mainly applying higher dosages than the recommended by the fibres supplier. Overall, the current results elucidated that implementing dedicated material studies at micro-scales can assist on understanding the material performance and tailoring systems beyond sometimes recommended reinforcement dosages by the suppliers. Finally, a semi-circular bending test was performed as the largest scale of this research using various fibre amount composition as well as fibre length inside the bituminous mix, and the final results mainly correspond with the other examinations that have also been conducted. Therefore, the research methodology utilised in this thesis has been able to examine the reinforcement effect brought by the integration of synthetic fibre to failure performance of the warm mixed asphaltic mixture specifically regarding the cracking resistance extensively.

Table of Contents

Table of Figures

1

Chapter One: Introduction

1.1 INTRODUCTION

An ever-increasing demand exists to produce durable asphaltic materials able to extend the life of pavement structures to meet the continually increasing traffic loads. In combination with the unexpected climatic changes, performance-related problems, such thermal cracking caused by the rapid temperature changes, or low temperatures, are more obvious leading to increased maintenance costs. Within this framework, road authorities, pavement scientists and designers have been considering technologies to reduce these problems by delivering more durable materials [1] and pavements [2] with improved performance. Therefore, various technologies have been proposed to improve the performance of asphalt pavements, and one of these is the utilisation of fibres as reinforcement in asphaltic materials [3]. Reinforcing with fibres, and mainly synthetic fibres have been used widely in asphalt pavements because of the capacity of synthetic fibre-reinforced systems to withstand additional strain energy before cracking, or fracture occurs and to add extra tensile strength to the material. In other words, these systems are able to retard the deterioration progress of pavements. This research is mainly focused on using aramid-polyolefin synthetic fibre as the reinforcement and their influence on Warm Mix Asphalt (WMA) performance are investigated through several tests in the mortar scale as well as full mixture scale.

1.2 WARM MIX ASPHALT (WMA) TECHNOLOGY

Warm Mix Asphalt (WMA) is a type of asphalt mixture that can reduce the mixing temperature down to 100-140^{0}C, which means approximately 30^{0}C lower than the standard mixing temperature of Hot Mix Asphalt (HMA). The first attempt of using lower temperatures in asphalt production came up in the 1950s, [4] then a modern improvement was introduced back in 1990s in Germany by using waxes to modify the viscosity of mastic asphalt. Hansen and Copeland (2013) recorded the significant increase in the use of WMA by 416%. Moreover, 26% of asphalt mixtures were produced by applying one of the warm mix technologies in 2012. Several techniques and technologies are invented to engineer the mixing temperature, namely by adding organic and

chemical additives or using water-containing foaming process. There are some advantages of WMA, as reported in the book of Zaumanis [5], below.

Environmental benefits, particularly due to the reduction of gases emission and lower energy consumption.

- Gas emission mainly comes from its production in the plant. According to data from Bitumen Forum, the amount of discharge at production temperature of 150°C is significantly low (1 mg/h), whereas below 80°C there is virtually no emission produced.
- Reduced fuel consumption is mainly related to the temperature reduction. Generally, WMA production can save the fuel consumption at 20-35% than HMA production. The save may bring into an economic benefit as well. A calculation performed by Zaumanis [4] resulted in 7-18% lower energy consumption by entire WMA production process, which was linked significantly to lower production temperature. The report NCHRP 779 [6] also indicated fuel savings of about 22%.

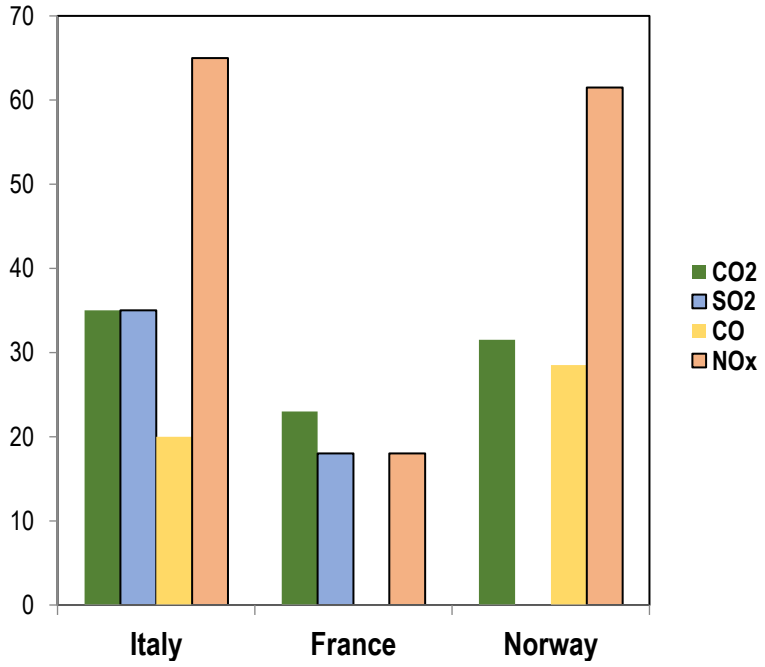

Figure 1.1. The amount of reduction of gas emission in some European countries *[7]*

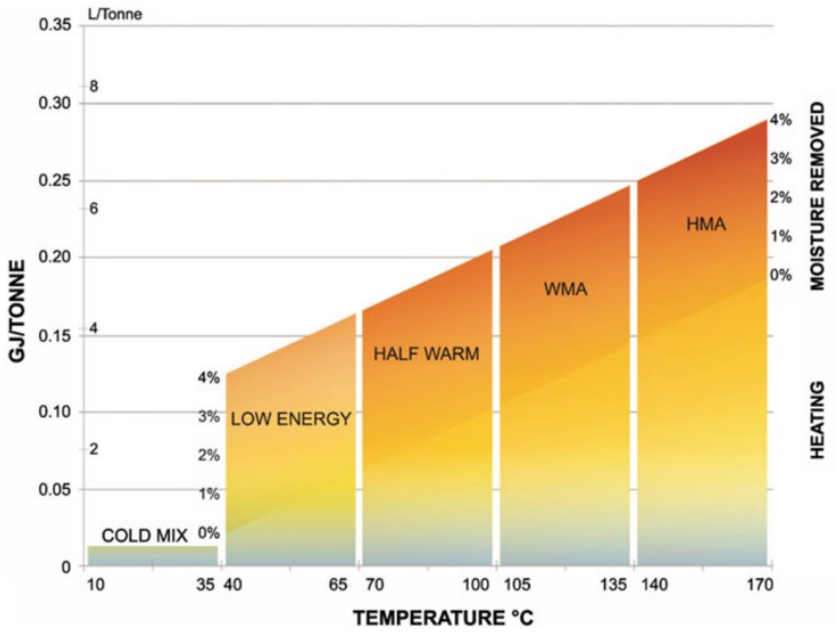

Figure 1.2. Comparison of reduction of fuel usage and reduction in emission *[4]*

Paving benefit (workability), this means that the window of compaction could be longer than that of HMA, due to the lower difference between mix and ambient temperature. Similarly, longer haul distance is possible for the same reason. Another benefit of the nondramatic temperature loss is also that the degree of compaction can be maintained significantly, which will lead to better density with the same or fewer roller passes in compaction. A case study developed in Germany has already proven the benefit, as the WMA construction process with working temperature of 102 to 139^{o}C could reach same density with a fewer number of rollers passes.

Production. The production using WMA technologies could lead to the increase of Reclaimed Asphalt Pavement (RAP) content in the mixture. This can be explained as when the mixing temperature is lower, more RAP content can be used without risk of undesirable ageing of the already stiff RAP binder. Moreover, less heating is also required for the virgin aggregate. However, certain things have to be taken into consideration in the production phase, as follows.

- Residual moisture may exist at the aggregates due to insufficient exposure level to the burning flame. However, the exposure can still be reduced to a certain degree. Another possible reason of residual moisture is as a result of foaming process. This can lead to the problem with moisture susceptibility.
- Lower temperature at the production may cause condensation in the baghouse, which results in corrosion and damp baghouse fines. Prowell et al. [8] have proposed some method to overcome the issue; preheating the baghouse, adding a duct heater, insulation, ensuring complete aggregate drying, etc.

- Another aspect regarding production is that more spaces are available to erect a plant site, due to its less emission, dust and noise.

Note that all the benefits vary depending on the type of production technology of the asphalt mix itself.

Furthermore, a report by Soto & Blanco (2004) and Els (2004) cited from the report made by Chowdhury and Button [9] has stated several extra values of WMA technologies compared to Cold Mix Asphalt, as follows.

- No curing time is required
- Better compaction than cold mix
- Possibility to use higher quality aggregate that cannot be used in cold mix
- Provide better mix quality due to proper coating and uniformity of the binder

Despite such benefits that are offered by WMA technologies, there are several major questions regarding the performance of this mixture; unfortunately, these issues have become enormous obstacles that delay implementation of warm mix asphalt in a large scale. Those can be elaborated as follows:

Water presence; the existence of water inside the mixture could be linked to the creation technologies of WMA, which are foaming and some chemical additives. This residual moisture due to incomplete vaporisation of water could lead to moisture damage, as it is also explained in the previous section. Another possible distress is premature rutting to the structure, as it was reported in several research papers that is linked to the moist in the aggregate.

Long-term performance; the word "long term performance" here is related to higher density and lower mix temperatures. Higher density due to higher compaction window, as well as low mix temperature, may generate insufficient air void, and issue with binder absorption as a consequence, that later result in problems with moisture, crack and ageing. [6]

Economical; the Economic issue is one of the major concerns of the developer, that prevents from the adoption of WMA technologies in mass production. Two major aspects related this issue are the investment or modification in the plant, and the extra cost for additives [6]. Therefore, it is necessary to prove the relationship between reduced energy consumption and reduced overall costs. Another possibility is to establish a strict rule against emission, which will induce the use of WMA.

Low-temperature behaviour; WMA might behave differently to a standard HMA in a low temperature due to the increase in both viscosity and stiffness of the binder. Zaumanis [5] stated in his book "Asphalt is Going Green" that this difference comes from the crystallisation of the waxes, which is one of the main technologies to produce WMA. Therefore, this factor needs to be taken into consideration.

One of the methods to overcome the lack of performance in an AC mixture is then to use fibre as a reinforcement, and this current research is trying to apply the fibre into the warm asphalt mix.

1.3 FIBRE AS REINFORCEMENT

Fibre has been considered as one of the primary options for reinforcement in the structural engineering field, both in concrete and asphalt mixture. In pavement engineering field itself, fibre has been used in an asphalt mixture since the early 1920s in the United States, as they used asbestos fibres. [10] The use of fibre in an asphalt mixture brings some general benefits regarding pavement strength and durability. The detail of advantages differs per each various of fibre, as well as their disadvantages. Therefore, the application of each fibre suits only for a certain asphalt mixture. For instance, cellulose fibre are used to reduce drainage ability of bitumen binder in an open-graded asphalt mix (porous asphalt/ZOAB and SMA), while other types of fibre are chosen to strengthen a dense-graded asphalt. The use of fibre in asphalt engineering has been known to bring several benefits to the asphalt mix, depending upon the type of asphalt mix itself (dense and open-graded). and fiber types and fiber adding amount. The benefits of utilizing fibers in asphalt mixes are presented below [11]

- Increase tensile strength (reduce cracking)
- Increase fatigue resistance
- Increase rutting resistance
- Increase durability (for higher bitumen content)
- Increase abrasion resistance
- Higher service life leads to potentially lower life cycle costs

All of these benefits can be summarised into two outlines: as a reinforcement for a dense-graded asphalt mix, and increase durability in open-graded asphalt by preventing drain down. There are five major types of fibre that are typically used in an asphalt mixture; each with specific advantages and disadvantages.

Cellulose fibres obtained from wooden plants, or sometimes from recycled newspapers are able to absorb bitumen, thus enabling a mixture to have a higher bitumen content. The special characteristic of cellulose fibres may be more suitable for an open-graded asphalt mixture to have a bit more bitumen content to increase its flexibility. There are several advantages, as explained in NCHRP SYNTHESIS 475 - 2015 [3], which are: increasing binder stability in open-graded asphalt mix, allow higher bitumen content in a mixture, widely available in an affordable cost, and eco-friendliness due to being taken from natural resource such as plants and other recyclable materials (e.g. newspaper). However, the addition of the fibre was proven to not provide any improvement of tensile strength to the mixture. Furthermore, the possibility to add an extra bitumen content brings also the potential of extra cost and rutting at high temperature.

Minerals that are used as a fibre are either natural (such as asbestos), or engineered products such as slag, basalt, brucite, steel, and carbon. [3] Previous research was conducted in TU Delft upon further use of steel fibre for induction healing of asphalt purpose. [12] However, according to Putnam [13], steel fibres are also prone to corrosion due to contact with water, which limits the long-term performance. The first type of mineral fibre that is used commercially was asbestos, back in the early 1920s in the United States [10], until it was prohibited due to health issue. [11]

The use of steel fibre was recorded by NCHRP SYNTHESIS 475 [3] to provide stability in an open-graded asphalt. Moreover, steel fibre was proven to bring self-healing property against cracks through induction heating. However, its susceptibility to corrosion could develop new issue inside the structure. In several cases, the mineral fibre may cause the mixture to be harsh and difficult to be compacted, which induce tire damage.

The most common type of polymer fibre is polyester, polypropylene, and combination of them. Different polymers have different melting points to be taken into consideration for creating an asphalt mix. This research is mainly focusing on the use of a combination of two kinds of synthetic polymer; aramid + polyolefin, which will be elaborated in the next section.

Figure 1.3. Cellulose (left) and mineral (right) fibres

1.4 SYNTHETIC FIBRES

Aramid, which stands for aromatic polyamide fibre, has comparable mechanical performances (tensile strength, compressive strength, fatigue capacity) to that of other popular types of fibre (e.g. steel and glass fibre) with a light density (1.44 g/m^3). Moreover, it is capable to maintain its properties even at high temperature, as its melting point is no less than 400^{o}C. These enable a broad range of application of aramid fibre, particularly in a hostile environment and/or lightweight structure. One branch of aramid fibres is Kevlar that can be used in various products, such as aircraft and automotive components (aircraft tires, brake pad, etc.), military equipment (body armour and helmet), also as ropes and cables – fibre optics, for instance. The term "aramid" refers to a manufactured fibre which is structured as a long-chain synthetic polyamide, according to the U.S. Federal Trade Commission. Each type of aramid fibres produced by different companies provide differences regarding its chemical structure, which leads to different performance and thus different possible application. On the other hand, polyolefin as fibre reinforcement material was firstly introduced by Montecatini in 1954, and only started to appear commercially in period 1970s. A polyolefin by definition of *Textile terms and definitions* [14] is a manufactured fibre which consists of a long-chain synthetic polymer composed of more than 85% by mass of ethane, propane or olefin units. According to European Association for Textile Polyolefins (EATP), there are two main components of polyolefin as synthetic polymers; polypropylene (PP) and polyethylene (PE), with PP by far is the most important.

1.5 HISTORY OF ARAMID AND POLYOLEFIN FIBERS

The history of the application of aramid fibre started at the 1930s until now, where two third of world's aramid production are held by Dupont with Kevlar ® as its trademark. The brief history of aramid are listed in **Table *1.1***.

Table 1.1. History of Aramid Fibre *[15]*

Year	Event	Producer
1938	Commercialisation of Nylon	
1962	Introduction, Nomex fibre	Dupont Co., USA
1965	Discovery of anisotropic polymer by Flory	
1970	Discovery of air-gap spinning	
1971	Introduction of fibre-B	Dupont Co., USA
1972	Introduction of Teijincorex	Teijin, Ltd. Japan and Dupont Co., USA
	Commercialisation of Kevlar	Akzo Chemicals BF, Netherlands
	Introduction of Twaron	Rhone-Poulene, France
	Introduction of Kermel	USSR
	Introduction of Fenilon	
1976	Introduction of SVM fibre	USSR
1978	Development of arenka aramid fibre	
1987	Introduction of HMO-50 aramid fibre	Teijin, Ltd. Japan
	Commercialisation of Twaron	Toyobo, Ltd. Japan
	Introduction of PBO-HM	Toyobo, Ltd. Japan
1996	Introduction of Trevar (discontinued)	Hoescht, Germany
1997	Kevlar 49HS by new fibre technology	Dupont Co., USA
1998	Introduction of Armos	Russia

The journey of Polyethylene started at 1920s when Hermann Staudinger introduced the concept of high molar mass macromolecules and defined the polymerization as the process that creates a covalent bond between individual small monomer molecules, although the first trace of PE was reported back in the 1890s by Pechmann as the side product of thermal decomposition reaction of diazomethane. The word polyethylene itself was firstly introduced in the work of a French chemist Pierre Eugene Marcellin Berthelot in 1869. 10 years later (1933), Fawcett and Gibson ran an experiment at the Imperial Chemical Industries (ICI) site in Winnington, England to investigate the effects of very high pressures (more than 1000 atm) on chemical reaction between

ethylene and benzaldehyde, only to found out a small amount (about 1 g) of an unexpected white powder coating the tip of the steel U-Tube used for the chemical experiment. Later they described the white powder as “waxy solid found in reaction tube”. Only two years after the discovery then he could unintentionally replicate again the reaction that forms PE since there was again a leakage that enables oxygen to infiltrate and decompose to provide free radicals which allow the formation of polyethylene. This product is nowadays called Low-Density Polyethylene (LDPE). The next major step was set back in 1951 when Philips was able to discover the catalysts (which were, nickel and chromium oxide/metal oxide on silica/alumina) to produce a High-Density Polyethylene (HDPE) under much lower pressure. Philips catalyst remains popular, which supply 40-50% of global production. Also around the same time (1953), Ziegler developed a way to use triethyl aluminium in so-called “Aufbau reaction” to produce ethylene oligomers and low molecular weight waxes or polymers. He found out the presence of nickel that changed the “Aufbau reaction” to yield 1-butene instead of oligomers, which would later be called “Nickel effect” by him. Then he registered two patents to the German Patent Office (German patent 973626 K. Ziegler) which claimed a method for the production of a high molar mass PE useful as plastic with an organo-metallic catalyst consisting of a trialkyl aluminium species and a transition metal compound. [16] These two technologies have continued to be the primary catalysts for HDPE for three decades until Kaminsky discovered a new compound called Methylaluminoxane (MAO) as an activator for metallocene catalysts. This catalyst was more suitable for polyolefin polymerisation, almost 100 times more active than Ziegler catalysts, and all these stepping stones have participated in the global production of PE fibre until today. [16]

Polypropylene (PP), in a way, share the similar history to PE fibre, as both PP and different PE products are based on a common monomer. [16] Thus, PP becomes the world’s largest polymer. Even though it is commonly said that PP was firstly examined by Philips Petroleum, no notable result could be collected until Hogan and Banks were able to invent a process to produce crystalline PP in 1953, based on the idea of modifying the catalyst technology (nickel oxide) developed by Philips with a small addition of chromium oxide. Another experiment attempted by Natta at Politecnico di Milano in 1954 has resulted in two patents in the same year, after exchanging the ideas with Ziegler. Then starting in 1957, the use of PP fibre was commercialised initiated by Montecatini with their Mopren products, until these days, and the data can be depicted from the graph below.

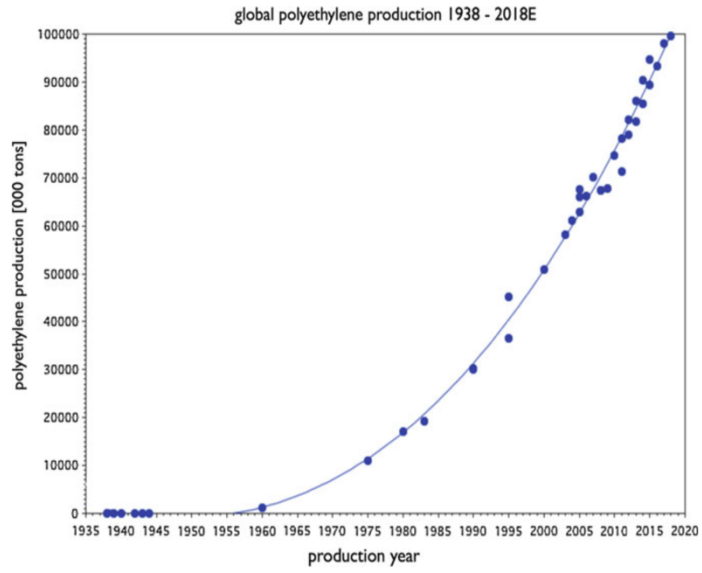

(a)

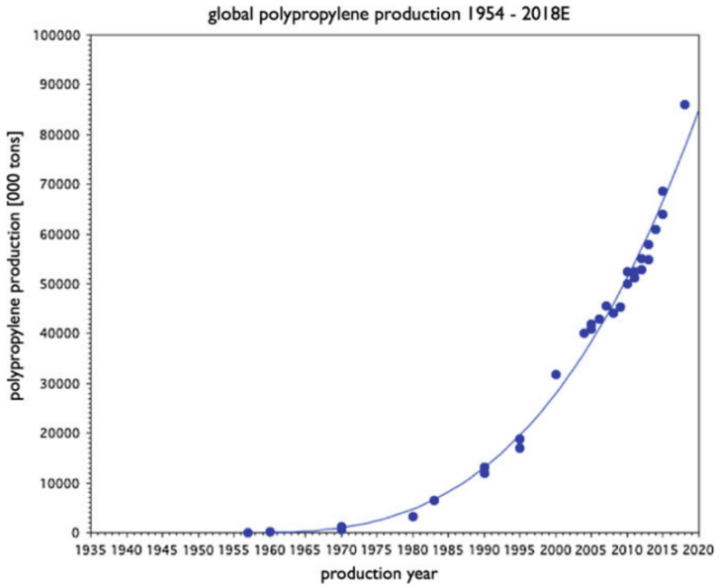

(b)

Figure 1.4. (a) Global PE production up to 2018 and (b) Global PP production up to 2018 *[16]*

1.6 PROPERTIES OF ARAMID AND POLYOLEFIN FIBRE

The production process of PPD-T Aramid fibre was explained in the book *Aramid Fiber of Poly Para-Phenylene Terephthalamide From The Netherlands* [17] as follows. Firstly, the condensation reaction between two monomers called 1,4-Para-Phenylenediamine (PPD) and Terephthaloyl Dichloride (TDC) form the end product with chemistry name as Poly Para-phenylene terephthalamide (PPD-T). **Figure *1.5*** illustrates the chemical structure of the PPD-T.

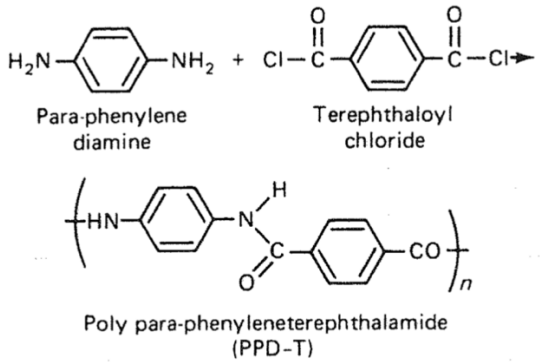

Figure 1.5. Chemical Structure of Aramid *[18]*

The polymer as the end product of this reaction then is washed to remove the acidic substance and later be dried. Furthermore, the dry PPD-T polymer is extruded from a spinneret inside a strong acid, mainly sulphuric acid >99.5%. The reason for using this liquid is due to its low price and high maximum solubility for PPD-T. [19] The polymer then rapidly coagulates and crystallise, forming its orientation and structure. Then the fibre is washed to remove the acid and neutralise its pH. Finally, the filament fibre is dried on steam-heated rolls. In this phase, the physical tensile strength is already fully developed. Looking at the chemical structure of PPD-T Aramid fibre, the aromatic ring structure contributes to high thermal stability, while the para configuration contributes to the stiffness of the molecules that leads to high strength and modulus. [18] Meanwhile, polyolefin structure can be defined as α-olefins with general formula CH2=CHx (x represents an alkyl group), which makes the chain asymmetric (exception can be made for PE). The brief chemical structure of both PE and PP are shown in **Figure *1.6***.

Figure 1.6. Chemical structure of (left) Polyethylene and (right) Polypropylene *[20]*

There are several aspects which can be taken into account when discussing the mechanical properties of an aramid fibre, as reported from various sources below.

Tensile modulus. Chang [18] and Jassal [15] give several data of this properties. For instance, the modulus of Kevlar29 fibre is 62 GPa, while Kevlar49, which is a modification of Kevlar29 by heat process under tension that increases crystalline orientation, has a modulus of 131 GPa.

Tensile strength. The breaking tenacity of a Kevlar yarn is 22 gpd [15]. This value is already more than twice greater than other polymer fibre products such as glass, polyester and nylon. Meanwhile, the post-processed Kevlar29 fibre will give break tenacity value of 23 gpd, which can

be translated as the tensile strength of 2.9 GPa. **Figure 1.7** presents both tensile modulus and strength of the fibre.

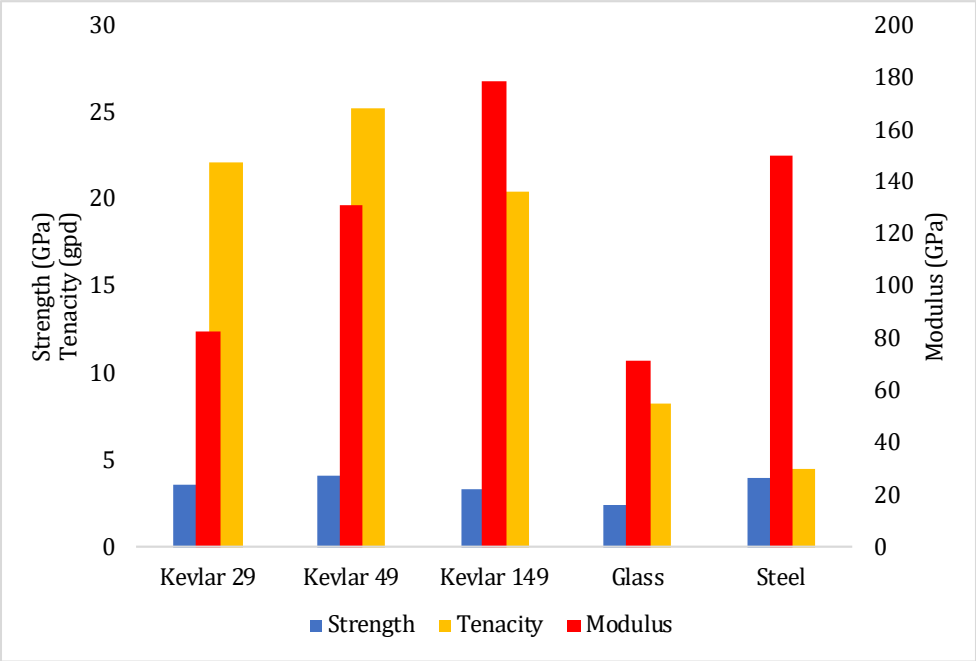

Figure 1.7. Mechanical properties of different aramid fibre [15], [18]

Temperature effect. According to Chang, [18] aramid fibre is insensitive to temperature changes. It is depicted from **Figure *1.8***, which indicate both the retained tensile strength and modulus to around 80% of its maximum capacity at high temperature.

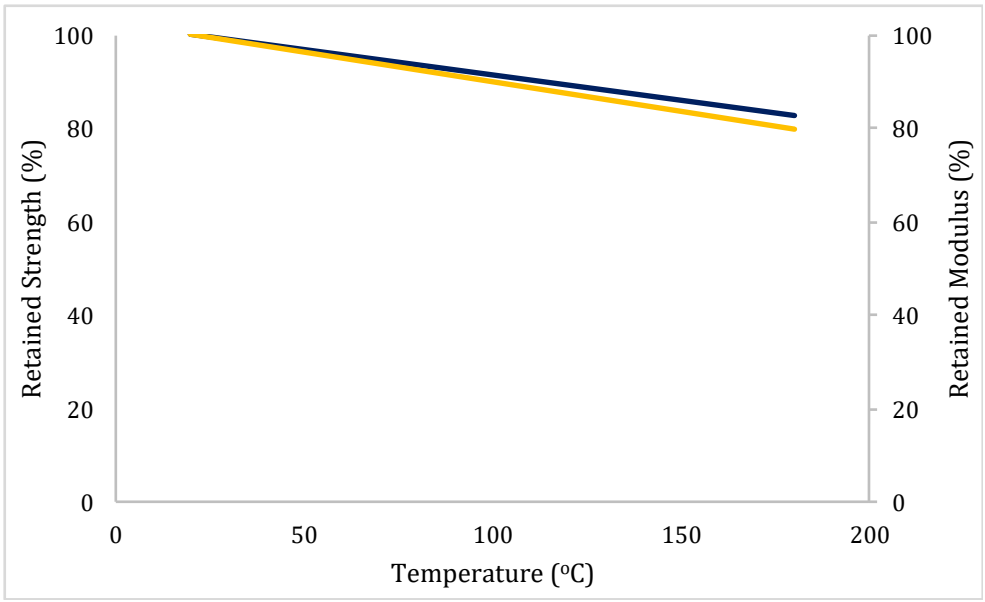

Figure 1.8. The effect of temperature to tensile strength and modulus of aramid fibre *[18]*

Fatigue. Fatigue properties of aramid may differ with respect to each failure mode. In terms of tension, aramid is reported to exhibit an excellent fatigue resistance; no observable failure even after 10 million cycles at the load of 60% its breaking strength. [18]

Compressive behaviour. Jassal [15] explained that aramid fibres behave elastically when subjected to tension. However, different behaviour is shown under compression or bending, as plastic deformation occurs in this stage with failure occurs at the strain of 0.3-0.5%, as shown in **Figure *1.9***.

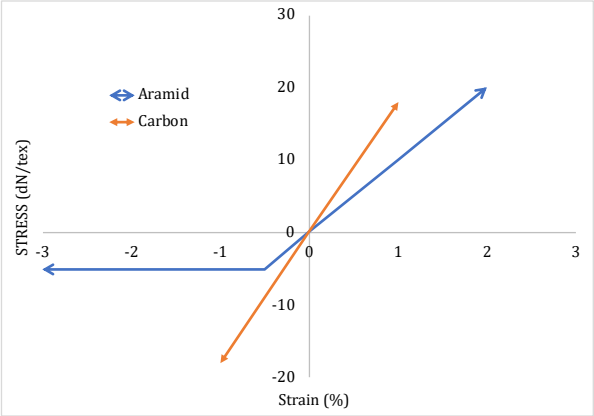

Figure 1.9. Tensile-compressive properties of aramid *[15]*

This phenomenon is known to correspond to the formation of structural defects named as Kink bands, which is related to compressive buckling of the aramid molecules. Therefore, the use of aramid as reinforcement in a compressive structure should be allowed only to a limited value. [18]

Polyolefin has, in general, great mechanical properties. For instance, a normal PP yarns have excellent resistance to wear as well as high shear strength. High bulk elasticity and dimensional stability enable PP to be used for various applications. Furthermore, PP has an excellent resistance to mineral acids and alkali, and it can be easily converted into precipitable gases. Consequently, PO fibres have certain advantages, such as good tensile strength, low specific gravity, chemically inert, high abrasion resistance, safe to human skin, non-water absorbent, and its ability to be thermally bond and form. The compilation of the mechanical properties of different types of polyolefin fibre is presented by **Table *1.2***.

Table 1.2. Properties of different polyolefin fibres

Properties	**Unit**	**Polyolefin type**		
		LDPE	HDPE	PP
Molecular weight	M	$(2\text{-}4)x10^4$	$>3x10^4$	$>10^5$
Specific gravity	kg/m^3	920-940	940-970	900-910
Melting point	^oC	115-122	135-140	162-173
Tensile strength	MPa	17-24	34-69	40-80
Modulus	MPa	140-210	550-1250	690-960

1.7 ARAMID-POLYOLEFIN FIBRE UTILIZATION

The initial use of aramid fibre was in the aerospace industry, which were keen to develop a composite structural part. Aramid-based product has been found out to be able to absorb 2-4 times as much energy and 25-30% better performance to carbon and glass fibre due to high specific strength and stiffness of the aramid fibre [15]. The hybrid composite of aramid and carbon fibre is hence commonly used in commercial aircrafts and helicopters. Another application of aramid is in tires due to high modulus and fatigue resistance, as well as good adhesion with the rubber; these characteristics enable it to be applied to conveyor belts. Furthermore, aramid has been used for ropes and cables to replace steel due to being light-weighted and stronger than steel; the strength of Kevlar (one type of aramid) in air is 7 times higher than steel, and 20 times higher in sea water. Not only the electro-mechanical cables and fibre optics but also cable system in structural bridges are the successful application of aramid fibre. Move to smaller scale, aramid fibre is use d for the fabricated suits of firemen, electric utility operatives as well as another safety equipment for workers such as safety gloves, due to high mechanical properties and thermal resistance. It can also be used in a bulletproof armour due to its good energy absorption, high mechanical properties and thermal resistance, thus able to protect its user from bullets from weapons and exploding munitions. [15] Kevlar chemical structure and orientation could enhance the wave propagation, which will increase the amount of material that is involved when handling any impact. It results hence in a higher energy absorbing capacity and dissipated energy. [15].

Polyolefin is known to be the polymer which is widely used as the ingredients of almost every plastic material (grocery bags, toys, etc.) that could be found. A report by IHS Chemicals recorded how much the popularity of polyolefin is nowadays: it accounts 62% of plastic materials, an exponential increase in respect to only 20% of the demand back in 1960; or more than 178million tons production in 2015. [16] This phenomenon is possible through its versatility combined with

the chemical (non-toxic, recyclable and low carbon footprint) and physical properties (polyolefin has low density, thus making a lightweight material possible) as well as its fair price. [21]

1.8 ARAMID-POLYOLEFIN FIBRE UTILIZATION IN ASPHALT

There have been numerous researches conducted worldwide to address the effect of aramid-polyolefin fibre to a bituminous mixture, among them discussed as follows.

Tapkin [22] has conducted Marshall stability and flow test as well as Indirect tensile test to examine the positive influence of addition of polypropylene fibre to an asphalt concrete mix. The mixture chosen was dense asphalt mix with 5.5% content by total mix weight of bitumen penetration grade 60/70 and maximum aggregate size of 9.52mm. Three different PP content (0.3%, 0.5% and 1%) were investigated. The research could draw several conclusions, such as an increase of 58% of stability and decrease of flow by 142% for the addition of 1% PP fibre, as well as higher fatigue life by approximately 27%.

Research by Kaloush et al. [23] in 2008 was noted as the first attempt to analyse the influence of aramid-polyolefin fibre combination in hot mix asphalt. Firstly, triaxial test showed the effect of the fibre to extend secondary stage and lower the permanent strain during the tertiary stage in a permanent deformation curve, thus meaning higher resistance against rutting. The same test with cyclic loading was able to examine the effect of temperature to the stiffness of the mix. The performance of Fibre-Reinforced Asphalt Concrete (FRAC) was distinctive mainly at high temperature, while at low temperature the stiffness is mainly carried by the mortar matrix. Secondly, ITT test exhibited the benefit of the fibre regarding thermal cracking resistance in every testing condition, with a notable difference of 25% and 50-75% for tensile strength and energy, respectively. Nonetheless, the effect of different fibre content infused to the asphalt mix was not noticeable in each testing temperature. Additionally, the use of fibre was reported to increase shear strength and energy, as well as fatigue life of the asphalt mix. The positive impact on fatigue life, however, appeared only at low strain level, which indicated that the fibre influences more at the higher traffic speed.

Another research in 2012 conducted by Stempihar et al. [24] concentrated on developing a feasibility study of Aramid-Polyolefin FRAC as the paving material for airfields. The paper itself compares the result of two different mixtures: the field samples from Jackson Hole Airport with 0.5kg/ton fibre content and from Sheridan County Airport without fibre, and one lab-designed mixture without fibre reinforcement by means of dynamic modulus (E*) test, four-point bending beam test, indirect tension test and Cantabro abrasion test. This research elaborated several benefits brought by the fibre. Triaxial test indicated that the addition of fibre enhances the stiffness of a mix, while ITT test revealed another improvement to the tensile strength and energy

with the value of 5-31% and 19-45%, respectively. Moreover, four-point bending test has shown various fatigue behaviour. Fatigue life of a FRAC is significantly higher than the standard mix at low strain levels, in particular at 600 microstrain; meanwhile, the result was almost similar at the highest strain level. Finally, Cantabro test reported that FRAC suffered a bit less loss compared to the normal mix, indicating a slight improvement to the ravelling resistance.

Ho et al. [25] evaluated the performance of two different mixtures: one only with polymer modified bitumen and another one with an extra of fibre reinforcement, after two-year review in Northern Arizona, USA. The specimens were extracted from the location and brought back to the lab to run bending beam rheometer and dynamic modulus tests. BBR test, which was used to measure thermal cracking, resulted in a higher relaxation modulus and lower thermal stress of Fibre Polymer-Modified Asphalt Concrete (FPMAC) compared to the normal PMAC, thus indicating the higher ability to do relaxation from the thermally-induced stress. The phenomenon can be linked to the melted and physically deformed polyolefin fibre that provide retarding viscosity to improve the low-temperature performance of the specimens. Moreover, dynamic modulus (E*) test concluded that FPMAC has a better rutting resistance than the normal PMAC due to its higher dynamic modulus. The field review performed by the authors has also confirmed these findings, as the FPMAC construction exhibits crack with an accumulative length of 11.6ft, almost 11 times lower than that of control mixture, while there is no rutting observed after two years of review in both constructions. Therefore, it is safe to say that the addition of aramid-polyolefin fibre brings positive impact both viscoelastic and dynamic behaviour of an asphalt mixture.

Takaikaew et al [26] recently used the same polymer fibre system to the hot mix asphalt with various types of binders, namely the normal AC60/70 binder and two types of modified ones (natural rubber and polymer modified). The research, which executed Marshall and ITT test, has proven the ability of a FRAC to significantly outperform the normal mix regarding tensile strength and stiffness, as well as rutting resistance and Marshall stability, regardless the means of the binder.

It was in 2016 that TU Delft and DIBEC joint to execute a research to examine the impact of the synthetic fibre to a warm bituminous mix. There were three standard tests performed according to the Eurocode with the purpose of compare the mechanical response of the FRAC to the normal mix regarding the stiffness and fatigue capacity, tensile performance and resistance to permanent deformation. A brief conclusion from the research suggested that the incorporation of aramid-polyolefin fibre indeed brought positive impacts to the performance of the specimen. The details of this research will be discussed in the next point, as also to explain how this research has established itself to provide preliminary objective of the current project.

1.9 THE INFLUENCE OF SYNTHETIC FIBRE ON DUTCH WARM MIX ASPHALT – TU DELFT AND DIBEC JOINT PROJECT (2016) *[27]*

This joint project has been established as a preliminary investigation for this current research to examine the reinforcing effect in warm asphalt mix by means of standard type tests. Several parameters, such as stiffness and fatigue life, indirect tensile strength and ratio of wet-dry strength, and resistance to rutting were measured. The examinations were executed using the standard dense asphalt concrete (DAC-16), with detail can be seen in **Table 1.3**

Table 1.3. Mixture specification (DAC-16)

Sieve Size [mm]	**Cumulative of agg. Passing [%]**		
	Lower limit	***Mix Composition***	*Upper limit*
22.00	100.00	**100.00**	100.00
16.00	94.00	**97.80**	100.00
11.20	75.00	**86.00**	95.00
8.00		**75.90**	
5.60	45.00	**59.20**	70.00
2.00	37.00	**38.10**	43.00
0.50		**16.00**	
0.18		**8.20**	
0.063	5.84	**6.10**	7.34
Bitumen (50/70)		**5.00**	

The production phase was handled by DIBEC, then the ready specimens were brought to the Pavement Engineering lab of TU Delft.

There were three standard tests conducted in the lab of TU Delft, namely 4-point bending test to measure the stiffness and fatigue capacity of an asphaltic beam specimen, triaxial test to characterise the resistance to permanent deformation, and indirect tensile test to quantify the effect of moisture to the tensile capacity of the specimen. All the details are to be discussed as follows.

Four-point bending test. This test was carried out following the Eurocode norm NEN-EN 12697-24 for measuring the resistance to fatigue and NEN-EN 12697-26 for the stiffness of a bituminous beam specimen. A beam with the measurements of 450x50x50mm of length, width

and height, respectively was subjected two different specifications of sinusoidal loading to measure two properties. The stiffness, which is defined by the value of stiffness recorded after 100 cycles of loading, was reckoned by using sinusoidal loading with various frequencies, ranging from 0.1 to 30Hz. Meanwhile, the test on fatigue was administered in three different strain rates (80, 120 and 200 ηm/m). The results are presented by **Figure *1.10***

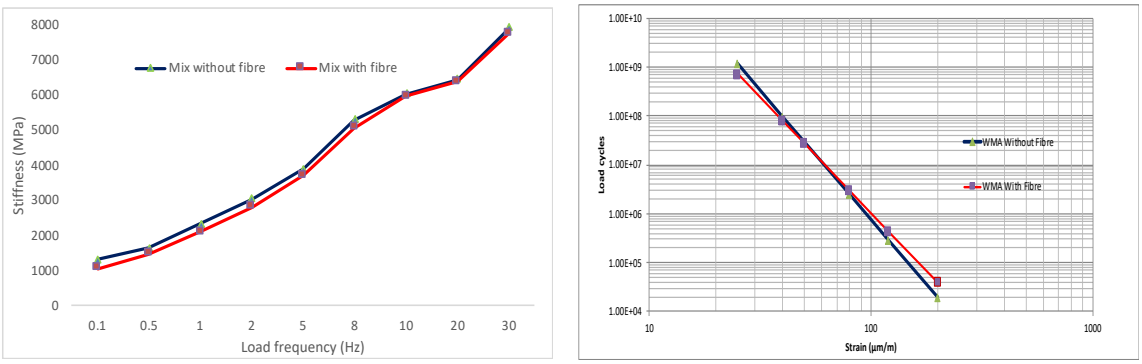

Figure 1.10. (Left) Stiffness result and (Right) Fatigue curve

Firstly, the stiffness between a normal and a fibre-reinforced asphalt mix was comparable, whereas fatigue life was slightly reduced by the incorporation of the fibre at low strain level and improved at high strain level. The low strain rate was used as the means to represent a higher traffic condition, whereas the high strain rate meant the low traffic ingestion or high-speed traffic. The outcome of fatigue life is in contrast to the report of Kaloush, which suggested precisely the opposite [23].

Triaxial test. The test was conducted based on the Eurocode NEN-EN 12697-25. The purpose of triaxial test is to measure the resistance of an asphalt mixture to permanent deformation. In this test, a cylindrical specimen of 100x60mm of diameter and height, respectively, was subjected to cyclic loading of up to 10000 cycles. The result presented in **Figure *1.11*** is a creep rate, taken as the slope in the permanent deformation curve from the cycle 1500 until 2000.

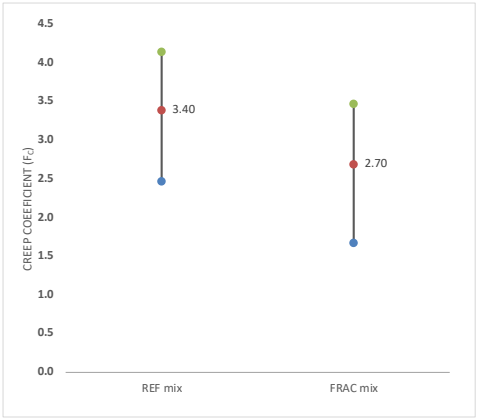

Figure 1.11. Creep coefficient (fc) taken from permanent deformation test

The creep coefficient resembles the permanent deformation that occurs in the mix within the given cycles. In this case, a higher coefficient indicates that the material has undergone more deformation when subjected to the loading. Therefore, the asphaltic specimen added with synthetic fibre showed a significant improvement to its resistance to permanent deformation, hence showing the obvious benefit of the incorporation.

Indirect Tensile Test (ITT). The examination aimed to observe the comparison of the tensile strength between a normal mix and FRAC mix, considering the effect of moisture. This test was performed in accordance with Eurocode NEN-EN 12697-12. A specimen with the diameter of 100mm and height of 50mm was firstly dried in a vacuum for 10 minutes, then soaked with a 40°C water inside a water bath for 68 to 72 hours. The soaked specimen was then mounted to the universal testing machine (UTM) which applied the monotonic tensile loading to crush the specimen. The final result is shown in **Figure *1.12***.

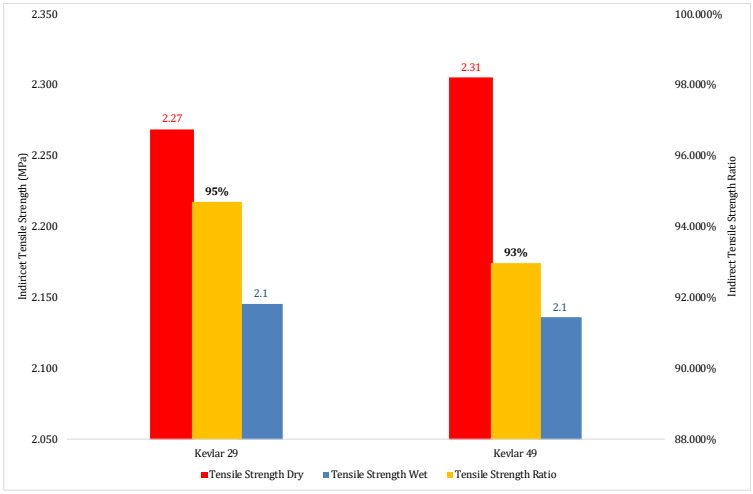

Figure 1.12. Tensile Strength (Dry and wet) and tensile strength wet-dry ratio

The influence of the inclusion of synthetic fibre to the tensile strength of a mixture is recognizable when moisture did not present in the sample. However, the effect of moisture was proven to be significant here, as the tensile strength of the FRAC specimen was equivalent to the control mix. This phenomenon was an indication that the existence of moisture was more critical to the strength of a fibre-reinforced warm asphalt mix. The explanation is that aramid in particular has been reported to have a tendency of absorbing moisture. [28] Nevertheless, the inclusion of synthetic fibre could still be inferred as to improve tensile strength of an AC mixture, which is coherent to the other research mentioned previously [26].

The tensile strength of a bituminous mix is associated with its resistance to crack, as well as fatigue capacity. Using the synthetic fibre, whose natural state is observed to be more suitable to provide reinforcement against tensile loading, is believed to improve this particular mechanical

response of the mix, as proven by the preliminary project of DIBEC and TU Delft [27]. However, the finding of Kaloush shows that, while the inclusion of fibre indeed is beneficial to a mixture's tensile resistance, the degree of improvement is independent of the dosage of fibre [23]. While the critical location for the tensile failure occurs in the interface of the mortar matrix, there has not been any research exclusively addressing the benefit brought by various synthetic fibre dosage and length to this mixture component, as well as the interaction between the fibre and asphalt mortar that is important to understand the reinforcement mechanism offered by the inclusion of the synthetic fibre. Moreover, there has been a finite resource about the effect of the fibre inclusion on the mechanical response of a warm bituminous mixture against tensile loading. This research hence tries to present the answer to providing a clear picture of the actual effect of the fibre addition, specifically to a warm asphalt mixture.

1.10 METHODOLOGY OF RESEARCH

The use of fibre in a bituminous mixture has been popular for ages and it is well known to have enormous influence on the mechanical properties of the mixture. The use of synthetic fibre in the mixture has become more common nowadays, with aramid and polyolefin are among the polymers. Aramid fibre has a wide range of applications, namely as a component in an aeroplane to the main material of bulletproof vests, and it is known to possess such a high tensile strength and high thermal resistance which is hoped to bring influences in the mechanical properties of an asphalt construction. On the other hand, polyolefin fibre is often used for textile products and, due to its low melting point, will disperse during asphalt production and provide better bonding inside the matrix.

The aim of this research therefore is to examine the behaviour of the combination of these two fibres inside an asphalt mixture starting from the fibre-matrix interface stress (by doing pull-out test) to the influence of the fibres to the tensile strength and fatigue life of the bituminous mixture (direct tension test on mortar sample and semi-circular bending test on the full-scale mixture). It helps one to characterise the behaviour of the fibre as well as its benefit as to increase the tensile strength as well as prolonging the fatigue life of the asphalt mixture, an upgrade that has always been deemed by most pavement engineers. Another goal is to obtain the optimum fibre content to certain environmental condition since both pull-out and direct tension test are executed in different temperatures to resemble the characteristic in both high and low temperature.

There are two types of bituminous mixtures produced in this research; one is an asphalt mortar, which is basically a mix between fine sand, filler, bitumen and the fibre; another one is the full-scale asphalt mixture with the specification of DAB-16. A combination of two different types of synthetic fibres, Aramid and Polyolefin, is used in this research, namely FORTA-FI®, under the

provision of Dutch Fibre Trading. There are three different fibre contents that will be examined; 0.05%, 0.1% and 0.5% of the total mixture weight. Moreover, the effect of fibre length on the failure performance is also addressed. The properties of the synthetic fibre are shown in **Table *1.4***.

Table 1.4. Properties of Aramid and Polyolefin Fibre

Physical Properties		
Aramid Fibres		
Length	19 mm	
Form	Monofilament	
Tensile Strength +	2758	Mpa
Specific Gravity	1,44	
Operating Temperatures	-73 - 427	^{o}C
Polyolefin Fibres		
Length	19 mm	
Form	Serrated	
Tensile Strength	N/A	*
Specific Gravity	0,91	
Operating Temperatures	N/A	*

* *Fibres will become plastically deformed during asphalt mix production*

+ 2758 MPa is applicable for 1 square inch (6.4516 cm^2) area of fibre

Another component is the chemical additive to make the warm asphalt mix provided by ANOVA 1502. The standard dosage of this additive specified by the manufacturer is 0.4-0.6% of total bitumen weight for normal bitumen, and 0.7% for a synthetic modified or very stiff bitumen, with an effect of temperature reduction by 40^{o}C. Furthermore, the use of this additive is aimed to enhance workability and compactibility of an asphalt mix, as well as enabling compaction at the lower temperature.

In this thesis, the explanation of the aramid and polyolefin fibre is given in detail in Chapter 1. The pull-out test case is presented on Chapter 2, followed by the examination of the tensile strength and fatigue life of an asphalt mortar using direct tension test on Chapter 3. The final chapter (Chapter 4) contains the investigation of the influence of the synthetic fibre on the tensile strength of an asphalt concrete mixture. The complete structure of the thesis is presented in **Figure *1.13***.

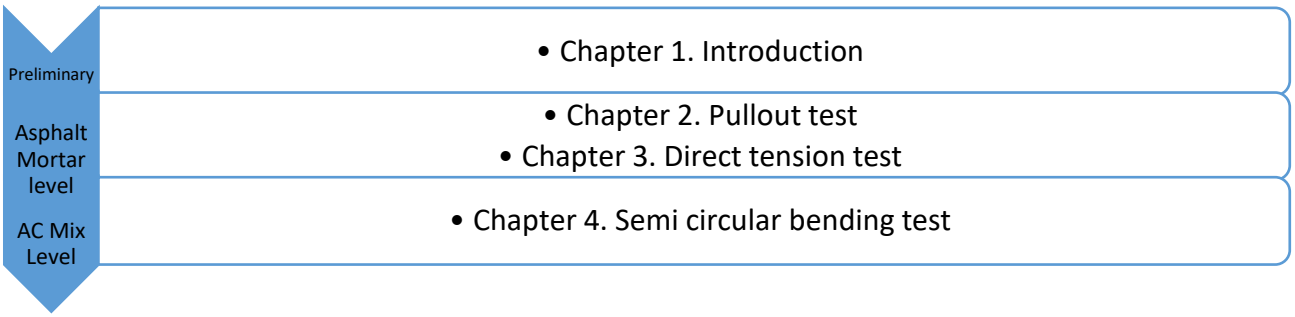

Figure 1.13. Thesis outline

2

Chapter Two: Fibre-Asphalt Mortar Interface

2.1. INTRODUCTION

One of the significant roles of both aramid and polyolefin fibre inside an asphalt mixture is to provide extra bonding capacity between binder and aggregates, as it was reported by Transportation Research Board. [3] Since aramid and polyolefin fibre is made for such purpose to provide additional bonding and tensile strength inside an asphalt mixture, it is necessary to perform such a small-scale test to measure bonding behaviour inside a mortar specimen by means of a pulling out test. The pull-out test is performed such that the friction between the fibre and the mortar could be quantified, hence the bonding of fibre inside an asphalt mixture can be predicted. The typical output of this test is mainly the stress-displacement curve, and the pull-out force is determined from the peak force in the curve.

The pull-out test has repeatedly been done to define the bonding between fibre and host structure. Research conducted by Rieger [29] as well as Markovich et al. [30] have succeeded to derive various bonding behaviour of a steel fibre inside concrete matrix with different parameters, such as w/c ratio and embedded length. Another research was conducted in TU Delft using Abaca fibre inside a concrete mixture by Sayed [31], with the result of a low bonding stress between the fibre and concrete matrix of 0.018 MPa. Another report by Park [32] analyse the interface matrix between pure bitumen PG64-22 and steel fibre. The research concluded three different failure mechanisms in respect to the environment condition, as shown in **Figure *2.1***: Matrix Failure (MatF), which means that the bitumen is pulled out along with the fibre, is the governing mode at high temperature (more than 20^{o}C) and/or slow loading speed. Interface Failure (IntF), which means that fibre is pulled out cleanly from the matrix, is the governing failure mode at low temperature (at -20^{o}C) and/or high loading speed. The third mode (MixF) is the combination of the first and second mode that occurs frequently at higher loading speeds at the temperature of 0^{o}C. MatF is characterized by a slow and gradual increase in the force after the peak while IntF exhibits a sudden drop after the peak. He was also able to develop a finite element model to illustrate and predict the interfacial behaviour of matrix-fibre.

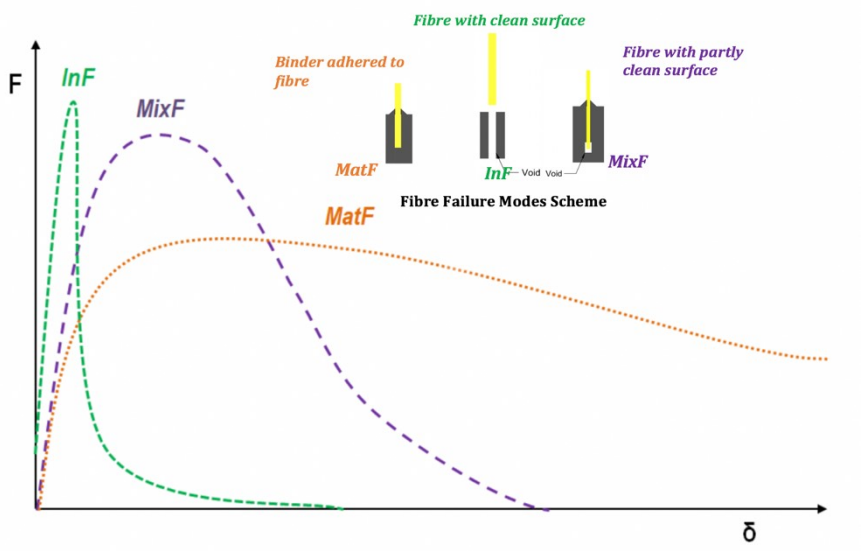

Figure 2.1. Scheme of different failure modes of pull-out test *[32]*

Further research specifically examining the aramid fibre has been done by Shunzhi et al. [33] to characterize the effect of fibre on bitumen and mortar level under low temperature. Both the bitumen and mortar were treated using hot mix technique and the tests were performed at -18°C. It was found out from the tests that aramid fibre had 5-7 times more pullout strength than that of polyester fibre. Furthermore, the suggested interface length between the fibre and bitumen matrix was 19mm, way more than that of polyester fibre, to fully activate its bonding capacity. Another phenomenon was that the pullout strength could exceed fibre strength, which is assumed as the effect of either bitumen or mortar that coat the fibre. In this present research, the bonding between aramid fibre and a warm-technology bituminous mortar will be examined. Furthermore, different conditions (temperatures and loading speeds) will be applied to the test to check the influence of those circumstances to the bonding behaviour.

2.2. METHOD AND PREPARATION

A warm mix bituminous mortar is prepared as the matrix, while the fibre is grouped to form strands. In the current studies, the reason for not using aggregate was to avoid the complication in determining the interface behaviour due to the influence of extra material. The specifications of the mortar can be seen in **Table *2.1***.

The fibre is grouped into strands by means of the weight of the group. This approach is used due to the difficulty in placing one single aramid fibre to this test. The weight of the strands is maintained to be (0.053±0.005) gr. The number of fibre in the strands can be therefore be back-calculated using the specific gravity.

Table 2.1. Asphalt mortar composition

		Density (g/cm3)
Sand	47.10%	2.595
Bitumen 50/70	23.80%	1.03
Filler (Wigras)	29.00%	2.595
ANOVA 1502	0.7% of bitumen weight	

The first step is to create the mortar using the prescription above. Firstly, bitumen is heated to 160°C while the other materials (sand and filler) are heated at 130°C for one hour. Afterwards, the Warm Additive is put into the bitumen, while sand also mixed with filler and fibre at their current temperature (≈130°C). Bitumen then is mixed with the other mineral components of mortar for around 7 minutes until the mixture is properly uniform. Finally, the mortar is poured into the split mould on both sides separately, and then unified right after the fibre is laid on top of either side. Initially, a brass tube with the diameter of 11cm, shown in **Figure *2.2*** (left) was split using a saw to create this split mould. This method is chosen due to its simplicity to keep the fibre placed in the centre of the specimen and to ensure the interface length while avoiding the fibre to bend inside the specimens. The samples, shown in **Figure *2.2*** (right), are then stored in a climate chamber in a temperature of ±13°C until they were used.

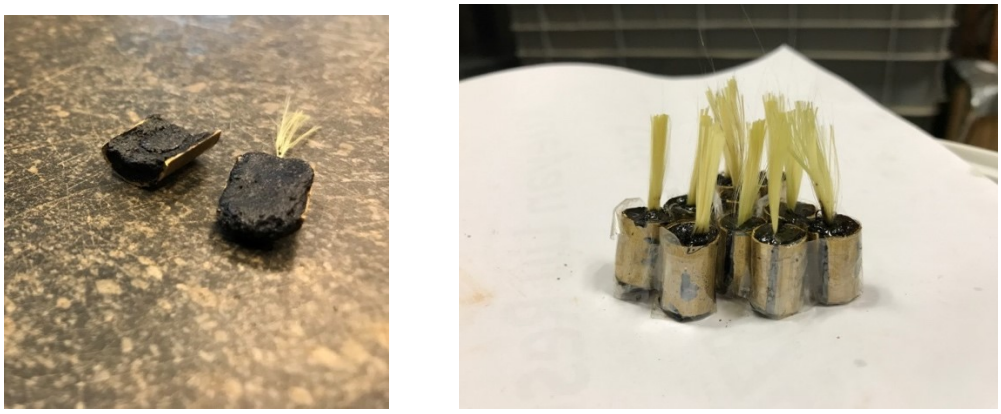

Figure 2.2. (Left) Split brass mould filled with mortar, fibre laid on one side and (right) the complete specimen

The examinations were firstly performed by using TS controller owned by the Material and Environment lab of TU Delft. The machine has a load cell with the capacity of 5kN, shown in **Figure 2.3**

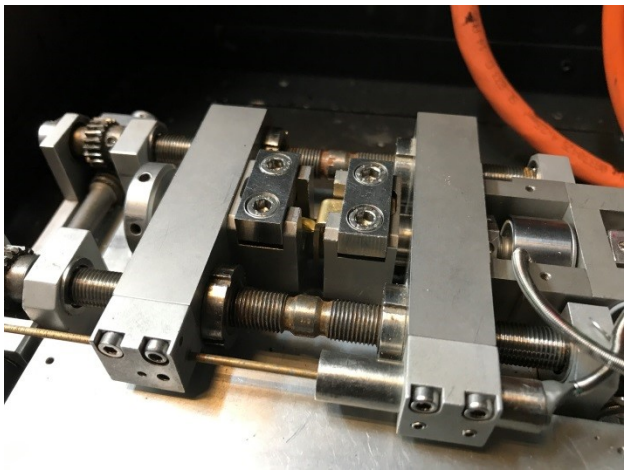

Figure 2.3. Tension controller equipment owned by Material and Environment Lab TU Delft

The apparatus was brought inside a climate cabinet owned by Pavement Engineering lab of TU Delft, which could go further to -20°C, and so is capable to create a -5°C testing environment. Unfortunately, the controller was prone to any moisture that could be formed due to the change of the temperature when the chamber was opened to mount the specimen to the clamping. The moistures jammed the electricity component of the machine, thus making it impossible to operate. Furthermore, there were numerous issues regarding the suitability of the specimen to the clamping system provided by the equipment. As the result, slip occurred to both sides due to the lack of clamping force, as shown in **Figure *2.4***

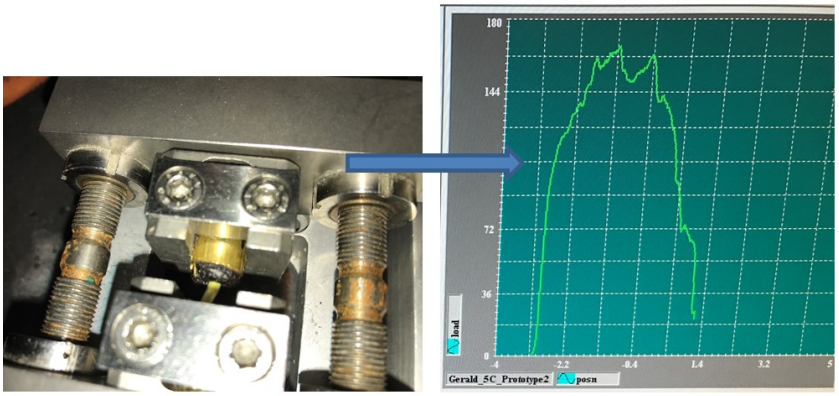

Figure 2.4 Clamping failure

Several patches were introduced to tackle the issue, namely two metal plates with extra grip on one side to clamp the fibre end, and a special-constructed brass clamp to the other fixed end. To add extra force, the fibre was also attached to the plates by creating a thin layer of glue. The whole patches can be seen in **Figure *2.5***.

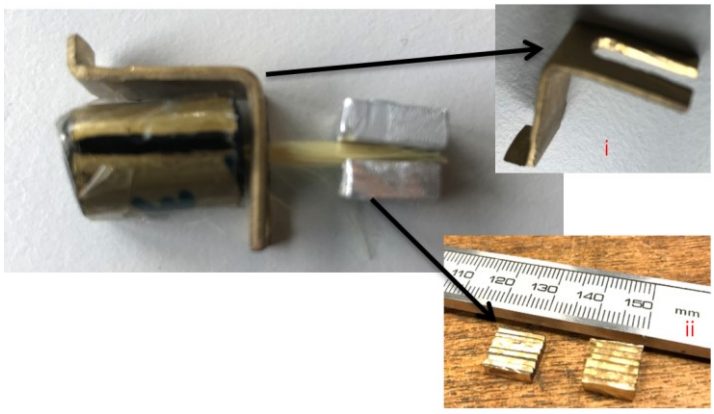

Figure 2.5. Pull out test extra clamping component: (i) special plate to hold the movement of the brass mould at one side and (ii) two plates with rough texture to clamp the fibre on the other side

The addition of extra plate to the mortar clamping system was meant to prevent any displacement that might have occurred to the specimen due to the pull-out force transferred from fibre end. A simple sketch of the forces governing at the clamping is shown in **Figure *2.6***

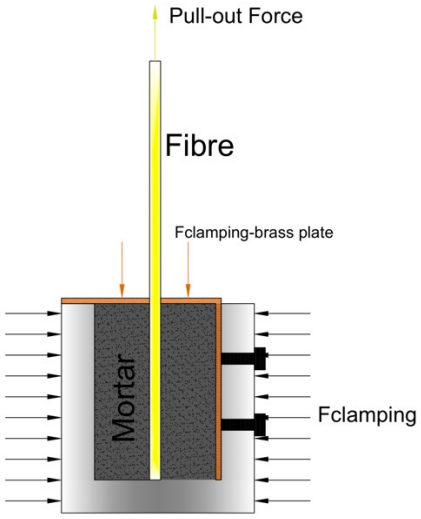

Figure 2.6. The sketch of forces acting during the test

These attempts however, did not end satisfactorily. The inclusion of an extra plate created a dilemma at the execution. Less confinement force applied to the clamping caused the whole system (mortar sample and mould + extra plate) to displace and slip out (shown in **Figure *2.7*** left part), since the clamping effect provided by the plate was dependent to the amount of clamping force given by the screws. On the other hand, increasing the clamping tend to provide an excessive confinement effect that could not be bear by the brass tube. As the result, the mould was crushed and brought damage to the mortar, making the clamping to be ineffective. This occurred ultimately at the high temperature, where the viscoelastic nature of mortar behaved to soften the matrix, thus making it easy to deform. The result is shown in **Figure *2.7*** (right).

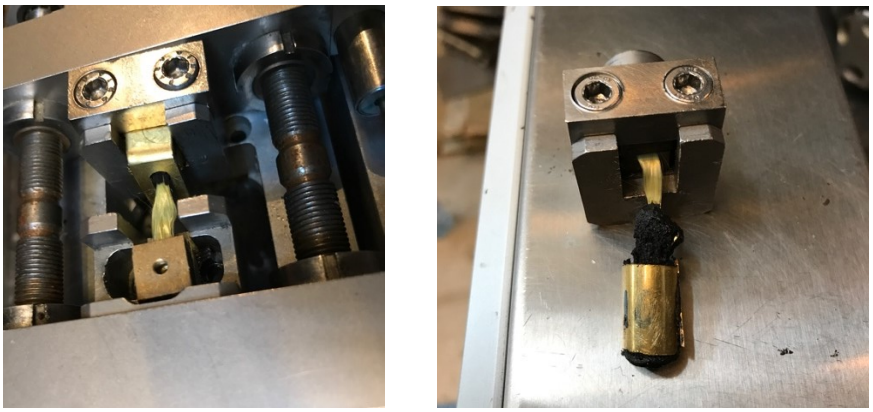

Figure 2.7. (Left) Displacement at mortar end due to less clamping force and (right) Broken mould due to excessive clamping force

The complexities of the first approach have made it inefficient to become the practical solution of a pulling-out test. Therefore, another approach has to be considered for the production as well as the testing and data acquisition.

To solve the obstacle, another split mould made of silicone is used to produce the sample. The production phase of these specimens is shown in **Figure *2.8***.

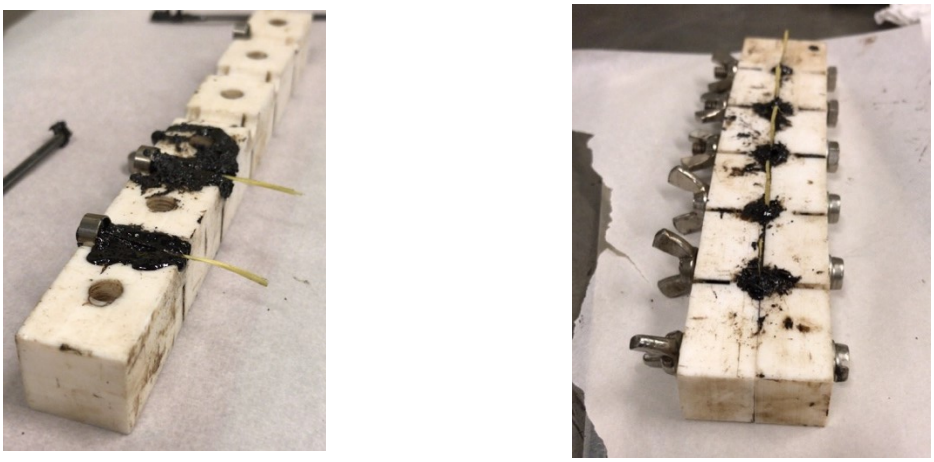

Figure 2.8. (a) Fibre is laid above the mortar poured to one side of split mould, (b) the specimen is ready to de-moulded

The preparation of the samples is exactly the same as described previously with the brass mould. The final form of the specimen therefore is shown in **Figure *2.9*** .

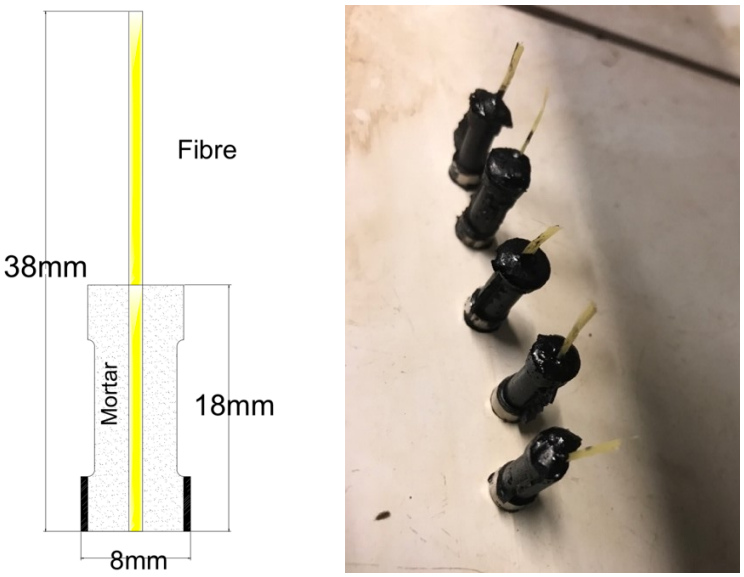

Figure 2.9 (Left) Sketch of a pull-out test specimen and (Right) Pull-out test specimen ready to be tested

The examination is executed using the Anton Paar Modular Compact Rheometer (MCR) 502 apparatus owned by Pavement Engineering lab of TU Delft, which is normally used to perform a direct shear rheometer test, can also be used for another purpose, such as for a tension test, as stated in the website [34]. A research by Mo [35] has accounted the use of the instrument specifically to measure the adhesion capacity of bitumen, by attaching it to stone columns The MCR machine has a load cell with the maximum capacity of 70N and limited displacement range of approximately 54mm due to the size of the testing chamber. The machine is linked to a computer using a special software in which the user could interact to modify the specifications of a test and capture the result. The whole setup is shown in **Figure *2.10***.

Figure 2.10. (Left) Anton Paar MCR machine + Data acquisition system and (right) specimen mounted to the clamping system

The specimen is designed in such a way to suit the clamping and chamber system of the MCR machine. Meanwhile, two special tiny plates have to be fabricated to patch the top clamp, since diameter of one strand of fibre is significantly smaller than the diameter of mortar. The two steel plates have a rough surface to maintain the clamping force on the fibre end. This is shown in **Figure *2.11***.

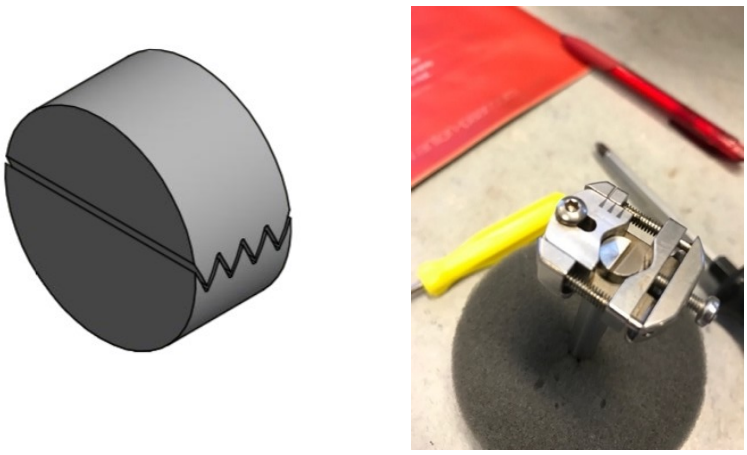

Figure 2.11. (Left) Sketch of extra plates and (right) Clamping system with the patch

The results generated are in form of force against displacement. The system apparatus enables the test to be carried in several temperatures. However, due to the limitation of loading capacity, the pull-out tests were performed only at ambient temperature with different loading speed. The observed effect is thus only regarding the different loading speed, which are 0.025, 0.05, 0.1 and 0.2 mm/s.

The output result of the test is a typical force-displacement curve, and the bonding strength can be obtained by use of following formulation.

$$\tau_{im} = \frac{2F}{\pi \cdot d \cdot l_e} \qquad \textbf{2.1}$$

where F is maximum load, d is diameter of one strand of fibre, and l_e is embedded length

The embedded length l_e is assumed to be the whole height of the cylindrical specimen, in this case is 16mm.

The maximum load is obtained from the load-displacement curve at the peak point of the load. That resembles the bonding characteristic between the fibre and asphalt mixture, considering the effect of temperatures and speed. Since bitumen has a viscoelastic property, its bonding capacity thus strongly depends on the testing temperature, while the pulling speed has to be also taken into account to the bonding strength.

2.3. RESULTS AND DISCUSSION

The interfacial characteristics of synthetic fibre-asphalt mortar system were examined by performing the same test at higher rates keeping the same testing temperature. It is observed that a higher loading speed resulted in a more brittle behaviour, illustrated by the rapid increment from zero to peak force and followed by a sudden failure right after the peak, where the increase of the loading speed is directly proportional to the results of the peak force. As shown in ***Figure 2.12***, the pull-out tested samples exhibited an increase of peak applied tensile load when the pull-out speed (displacement rate) was increased at the test ambient temperature (i.e., 29.5°C). For the fibre-asphalt mortar systems, the mortar part is characterised by a soft matrix due to the viscous dominant behaviour of asphaltic material at this temperature. In combination with the synthetic fibre as the one studied herein at the same temperature, the adhesion between fibre-matrix was enhanced and the matrix-type cohesive bonding has become the weakest part of the connection, and thus the governing failure mode. There are several mechanisms available to sustain the adhesion. Adhesion will occur so long as there is a contact between two substances at the molecular level, as well as the ability of the adhesive binder to infiltrate through the surface area of the fibre to provide a coating and, as a result, a mechanical interlocking. These confirm the same effects reported by Gao [36] .

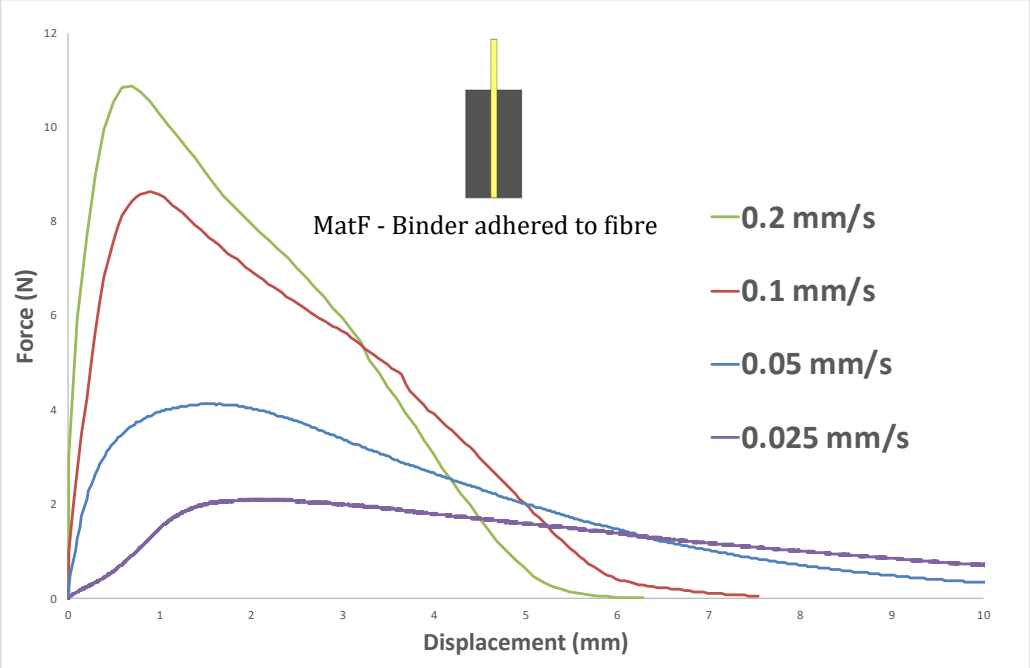

Figure 2.12. Force – displacement graph of the pull-out test at different loading speed

The phenomena could also be seen physically through the shape of the specimen at the failure state, as captured clearly in **Figure *2.13***. At higher loading speed, a brittle behaviour is exhibited and thus only small deformation is governing until the specimen fails. In contrast, the mortar part becomes less brittle when subjected to lower loading speed. As the result, more deformation is possible.

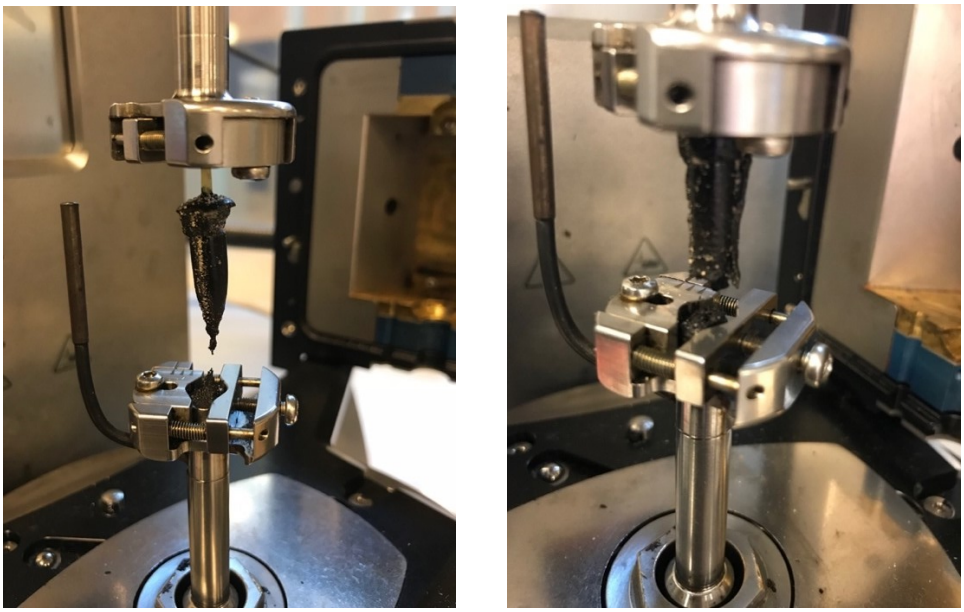

Figure 2.13. Failure mode of the specimen at (Left) low loading speed and (right) high loading speed

Both pictures show the failure to occur at the mortar near the bottom clamp, whereas fibre pulls the remaining matrix while subjected to the external force. This indicates that the matrix failure (MatF) is the only failure mode in the observation. Whilst the only failure mechanism in this observation is matrix failure (MatF), it is possible to perform studies on the reinforcing effect of the fibre to the other component of an asphaltic mixture. The fibre is capable of transferring the subjected tensile force to the matrix with a strong interfacial bonding capacity in order to activate the cohesive failure of the mortar as being the weakest link in the system, indicating that the bonding strength between fibre-matrix must be significantly stronger than the cohesive strength of the mortar matrix.

Finally, the calculation of effective perimeter and subsequently the shear stress generated through the pull-out test is not possible. The reason behind the impossibility is the failure mechanism itself, which is not caused by the failure of the adhesion of fibre-mortar, but rather caused by the cohesive failure of the mortar part. Hence, the attempt to convert the pull-out force to a shear stress based on equation ***2.1*** is not the best approach to explain the interfacial stress, as it is also explained by Park [32] that the shear stress in matrix failure mode is far below the critical

interface stress, although the stress may rise when a higher loading speed is governing. Therefore, the results were plotted as the peak force reached under the different displacement rates.

2.4. CONCLUSIONS AND RECOMMENDATIONS

The interface failure of fibre-asphaltic materials regularly occurred as the consequence of weak bonding between the mortar matrix and the foreign object added to the mixture, in this case, the synthetic fibres. Herein, the interaction of fibre-matrix was assessed by performing pull-out tests at room temperature, showing a cohesive or a matrix-type of fracture (MatF). A difficulty to reach the failure at the interface of fibre-matrix (IntF) mode is demonstrated, and therefore further studies should emphasise more on broadening the testing temperature to study more about the interfacial interaction of fibre-reinforced asphaltic systems. This is in order to achieve a better understanding in terms of bonding strength by having an interface failure mode during the observation. Nevertheless, it is clearly seen that a significantly high pull-out loading speed yields a higher brittleness level of the specimen at the given testing temperature. Meanwhile, the results of the current test have indicated that the adhesion between mortar-fibre is significantly stronger than the cohesive strength of the matrix. This suggests the positive impact regarding the effect of the incorporation of synthetic fibre to the mechanical response of an asphaltic specimen, ultimately at a high temperature.

3

Chapter Three: Fibre Reinforced Asphalt Mortar

3.1 INTRODUCTION

The tension resistance of an asphalt mixture is a critical parameter of its properties, due to its correlation to fatigue and crack resistance. The current standard test on tension capacity of an asphalt mixture is performed as an indirect tension test with a cylindrical shape sample compressed diametrically. The compression load then creates a tension stress at the centre part of the sample, which will lead to the tensile crack along the diameter of the cylindrical specimen. However, in this investigation, a direct tension test was utilized to examine the tensile capacity of a specimen. The initial application of a direct tension test came in form of a cylindrical sample being pulled in a uniaxial direction, performed by Bolzan et al [37]. However, this application had encountered a major issue in terms of the failure location, which was unpredictable and could even occur near the end cap (**Figure *3.1***). This kind of unpredictable failure location was not beneficial to the test and could damage the equipment.

Figure 3.1. A direct tension specimen with failure occurring nearby the end cap *[37]*

In order to localise the tensile failure to occur at the centre part of the specimen, Erkens and Poot [38] initially proposed a method to perform a direct tension test with such a sophisticated specimen geometry, appearing in a shape of a dog-bone. The hypothesis has been strengthened

by a study of finite element analysis performed by Kringos et al. [39] using a software named CAPA3D, in which the angle of the curvature plays a considerable role in influencing the inhomogeneous stress distribution with the deviation of up to 10% at the angle of 20°. **Figure 3.2** explains the finite element analysis and result.

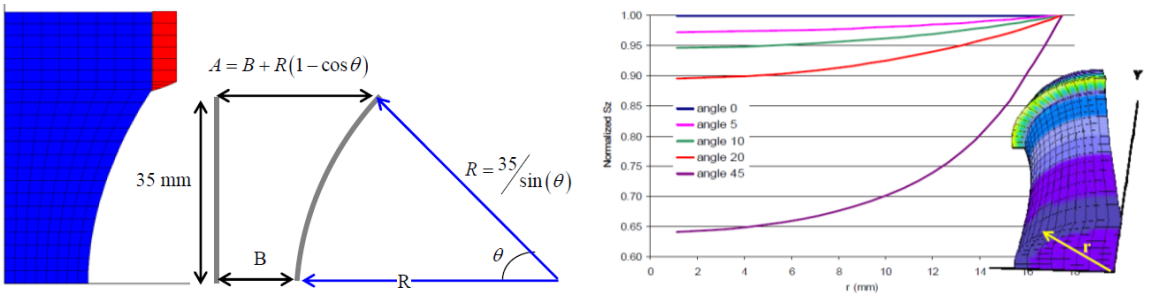

Figure 3.2. (Left) The definition of the angle of curvature and (Right) Effect of angle θ to deviation of stress along specimen length [39]

Apostolidis [12] later used the same method in his research, using the mortar composition (normal mix without coarse aggregate) to examine fatigue resistance and self-healing capacity of an asphalt mix. Another application of direct tension test is on bitumen level. Huang et al. [40] did the test with the goal to study the effect of mastic stiffness and degradation to the tensile strength of an asphalt concrete mixture. Meanwhile, Leegwater [41] conducted the test on the same level with the purpose to assess the self-healing capacity of asphalt. Therefore, this research aims to examine the effect of fibre to the mechanical performance of an asphaltic specimen at mortar scale by means of the parabolic shape sample. A CT-Scan is also initiated to get a better understanding over the distribution of fibre inside the body of a specimen, as well as the interaction between fibre and other mortar components.

3.2 METHOD AND PREPARATION

Warm asphalt mortar specimens, which are formed in the parabolic shape using a silicone mould, are prepared for this test. The test samples were produced by the following procedure. Firstly, ovens are heated to 130 and 160°C, respectively. Aggregates and fibres, which are placed in cans, are heated to 130°C while the bitumen is heated in 160°C. The aggregates and fibre are mixed while the additive with a prescribed dose is added to the bitumen. Afterwards, they are mixed together to finish a mortar mixture. These mixing processes are taking approximately 6.5minutes. The mixture then is placed back in the oven for a couple of minutes to reheat it along with the mould to 130°C. The purpose of reheating it is to maintain its workability since the mixing is performed at room temperature. Finally, the mixture is poured into the mould, as shown in

Figure *3.3*(a), which will create six samples at once. The mould, now filled with the mix, is then stored at a climate chamber and then a freezer until the specimens could achieve a reasonable stiffness which enables the de-attachment without being prone to damage or deformation. They are then placed in a container on top of a layer of sand, which provide support to the specimens and maintain their shape, since it is critical not to get any undesired deformation ultimately in the centre diameter of the sample in which the failure location is prescribed. This is shown in **Figure *3.3***(b). The composition of the mortar specimen is described in **Table *3.1***.

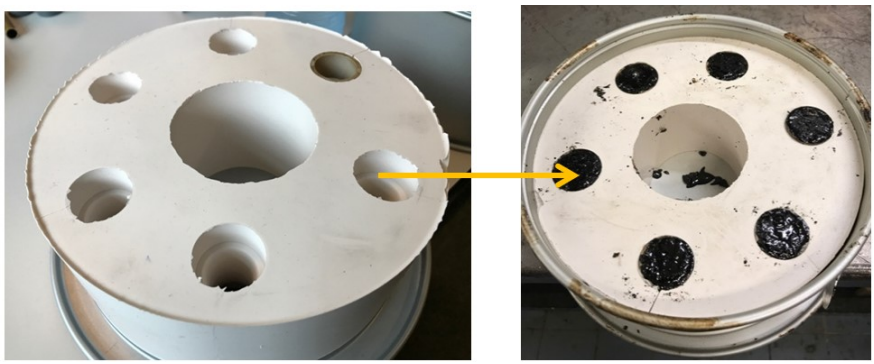

(a)

(b)

Figure 3.3. (a) The silicone mould ready to be poured with mortar and (b) mortar sample after demoulding

Table 3.1. Components of mortar

		Density (g/cm3)
Sand	47.10%	2.595
Bitumen 50/70	23.80%	1.03
Filler (Wigras)	29.00%	2.595
Fibre (38mm)	0.05, 0.1, 0.5% of total mix weight	1.44 (aramid); 0.91 (PE)
Fibre (19mm)	0.05, 0.1, 0.5% of total mix weight	1.44 (aramid); 0.91 (PE)
ANOVA 1502	0.7% of bitumen weight	

Universal Testing Machine (UTM)25 which has the capacity of 50kN and a set of data acquisition instrument, owned by Pavement Engineering lab of TU Delft, have been capable on executing the whole direct tension test. The temperature cabinet is able to render up to -20°C as its lowest temperature. The UTM is shown in ***Figure 3.4***.

Figure 3.4. UTM25 + Data Acquisition System

The now-ready specimens are subjected to two different tests: crush test with a monotonic loading and fatigue test with cyclic loading. The crush test is performed in three different temperatures (-5°, 5° and 20°C) and a displacement rate of 0.1 mm/s, taking into account three different fibre contents (0.05%, 0.1% and 0.5%). In order to study fibre length effect, specimens with shorter fibre (19mm) are also tested at the same conditions.

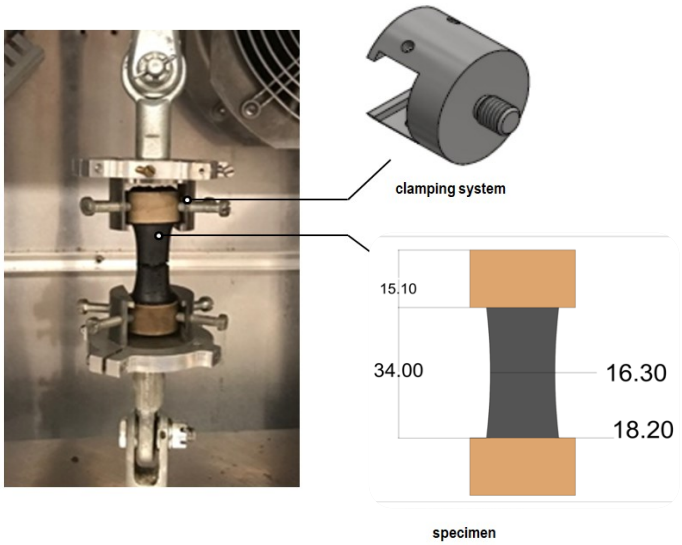

Figure 3.5. Direct tension test testing setup

The result of monotonic tests, which basically is a series of force-displacement data shown in **Figure *3.6***, can be converted to stress-strain data by means of following equations:

$$\sigma = \frac{F}{1/4\,\pi d^2} \qquad \textbf{3.1}$$

where d is taken by the smallest diameter of the sample that is located in the middle of the specimen, and the result is called engineering stress and the corresponding strain is defined by

$$\varepsilon = \frac{\Delta l}{l_0} \qquad \textbf{3.2}$$

In which Δl is the displacement of the specimen recorded in the test, and l_0 is the initial height of the specimen.

These results then are post-processed to build stress-strain curve. Finally, the peak strength and the total amount of fracture energy of the test can be determined. The term "energy" is obtained by means of the total area under the stress-strain curve and simply explained by following equation:

$$U = \int_0^{\varepsilon} \sigma \, d\varepsilon \qquad \textbf{3.3}$$

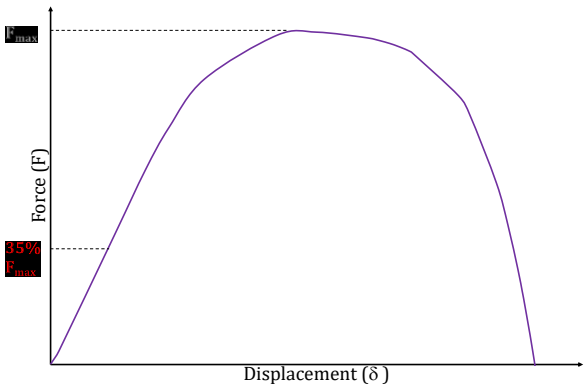

Figure 3.6. Schematic of a force-displacement curve of a specimen under monotonic tensile loading

The next step is the fatigue test. The tests are carried at one temperature (5°C) with loading frequency of 5 Hz, and the load level is determined by 35% of the peak load (**Figure *3.6***) for the lowest cases on different fibre contents in monotonic test results. The loading is shown schematically by **Figure *3.7***. The goal here is to observe the influence of the fibre to the fatigue performance of a mortar mix. Fatigue life is determined as the maximum cycle in which the sample fails.

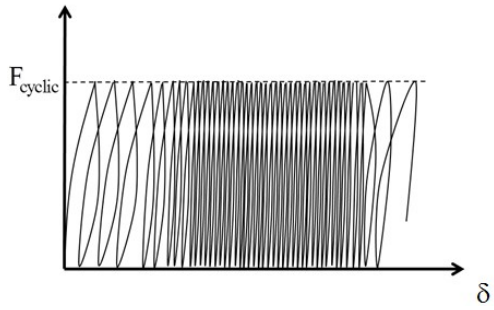

Figure 3.7. Loading scheme in cylic fatigue test

3.3 CT-SCAN OF DOG-BONE SPECIMEN

The X-Ray computed tomography (CT) scanning, which initial purpose is purely in the medical field, has been widely used in the pavement engineering scope nowadays. The major use, according to Nielsen [42], is to analyse the aggregate particles as well as voids in the mastic and mixtures. CT-Scan is performed with the help of Applied Earth Sciences Lab of TU Delft by using the Nanotom CT-Scanner from Phoenix|x-ray Systems+Services Inc, as shown in **Figure *3.8***.

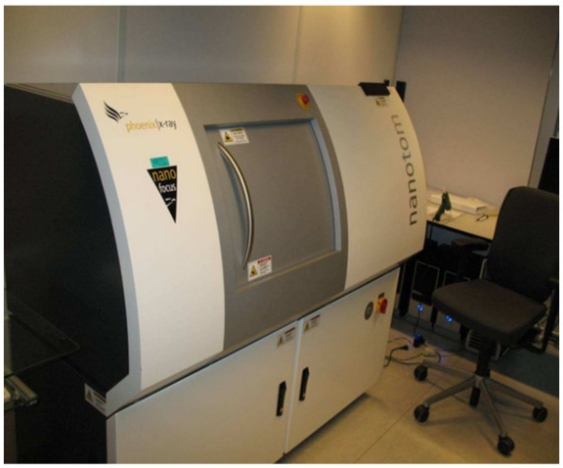

Figure 3.8. Nanotom CT-Scanner in Applied Earth Sciences Lab TU Delft *[43]*

The mechanism of a CT-Scanning, which is also portrayed in **Figure *3.9***, has been explained by Liu [43] as follows. A high power nano-focus X-ray tube emits a series of x-rays at different angles for each time after a small rotation of the sample. A series of two-dimensional images of the sample are then captured by the data capturing device, where the contrast of a scanned image depends on differences in X-ray absorption that is related to the densities of each component of the specimen.

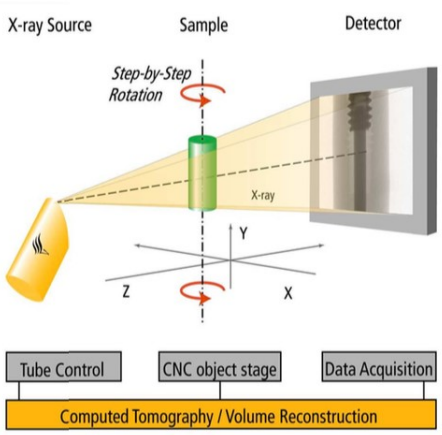

Figure 3.9. The mechanism of CT-Scan process *[43]*

The CT-Scan is performed in this research with two goals. The first aim is to examine the distribution of the fibre inside the body of the specimen. Several slices of the cross-section of a specimen thus have been made to solve the quest. ***Figure 3.10*** shows the CT-Scan result for the first goal.

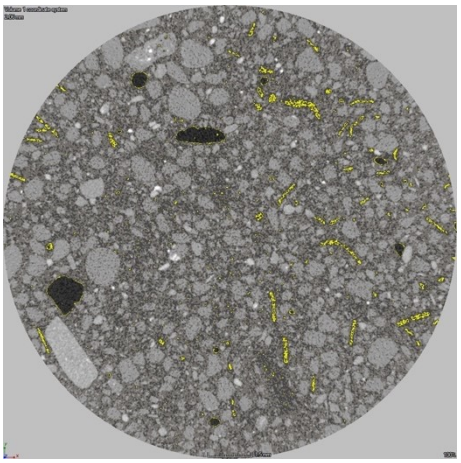

h = 2.06mm

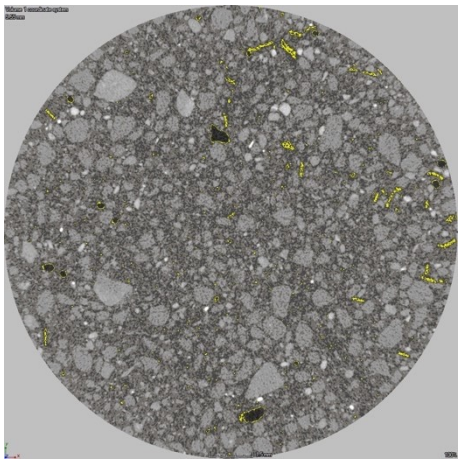

h = 5.55mm

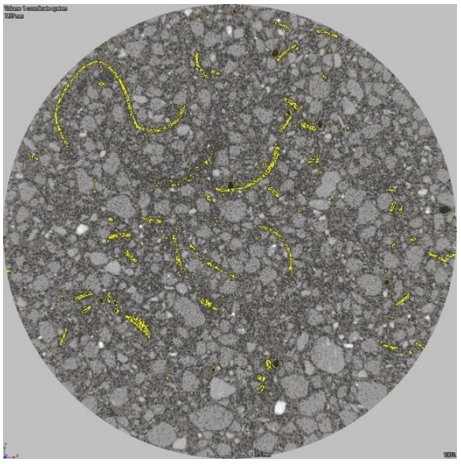

h = 7.37mm

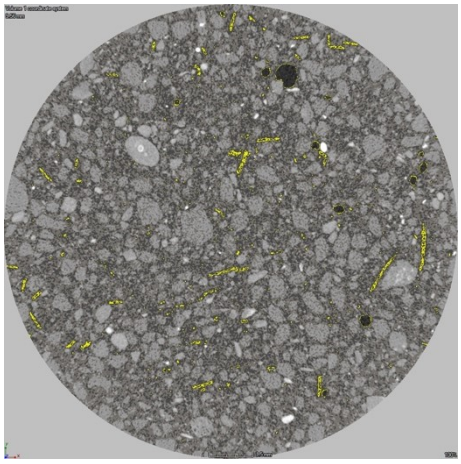

h = 9.56mm

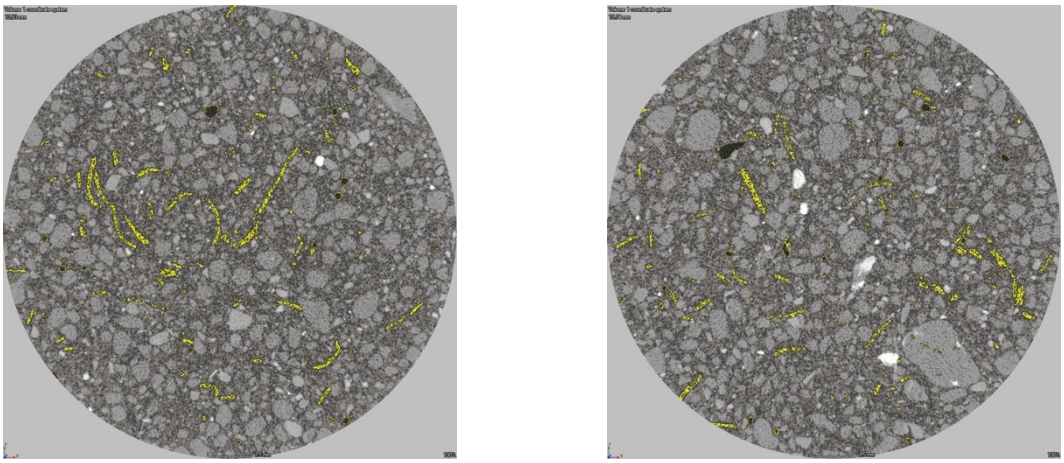

h = 10.93mm h = 15.54mm

Figure 3.10. CT-Scan result of a cross section of mortar specimen at different heights

It can be observed from the images that the distribution of fibre is not exactly equivalent throughout the body of the specimen. The main factor of this phenomenon is the mixing and pouring technique, which has to be executed manually. The distribution of the fibre, ultimately at the critical or failure location, could highly influence the result of the tension test, since tensile loading will generate a localised damage. While the distribution is assumed to be uniform through the whole body, such deviation is inevitable mainly due to the limitation of the production technique.

Secondly, CT-Scan is done to a specimen before and after the tension loading test in order to get a better understanding towards the interaction of fibre-mortar during the test. The marked area in the images, shown in ***Figure 3.11***, have captured the adhesive failure of fibre-mortar interface, in which a part of the fibre is displaced from the initial location, triggering a microcrack to occur.

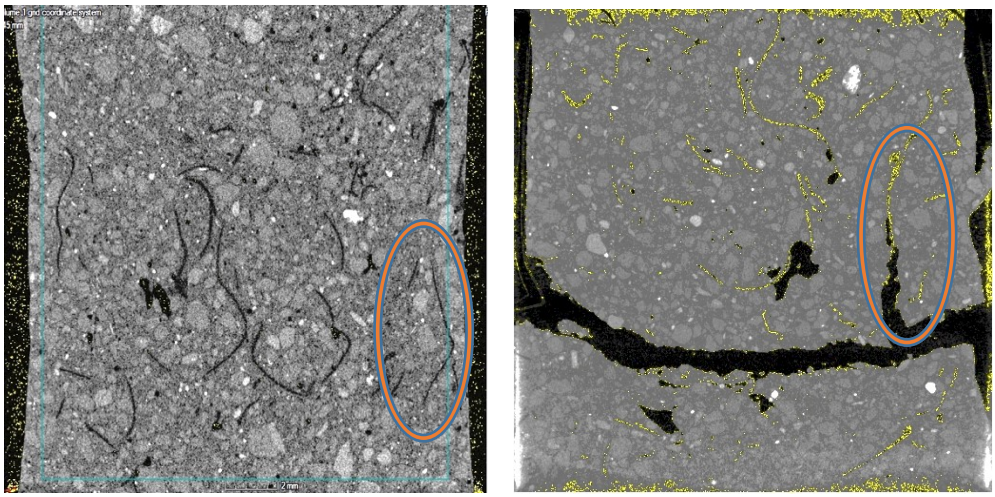

Figure 3.11. CT Scan of (left) undeformed sample and (right) the already cracked sample

3.4 RESULTS AND DISCUSSION

The tests are divided into two parts: the monotonic failure and cyclic loading fatigue test. The two results obtained by the monotonic failure test are tensile strength and total fracture energy.

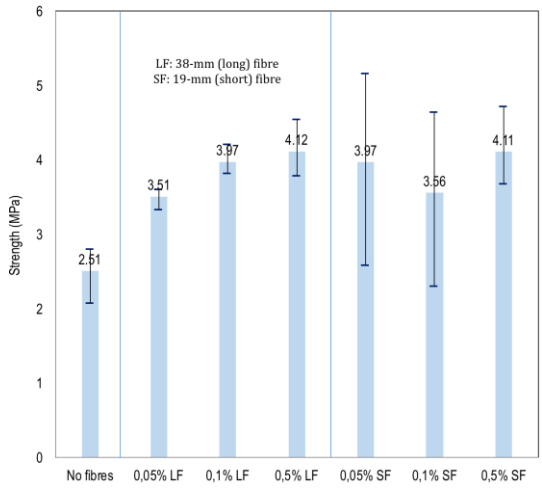

(a)

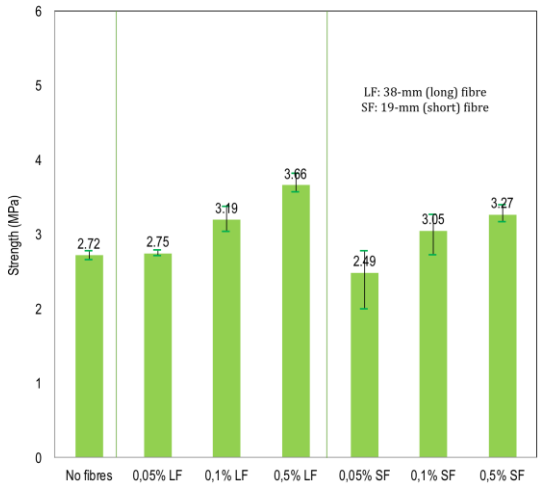

(b)

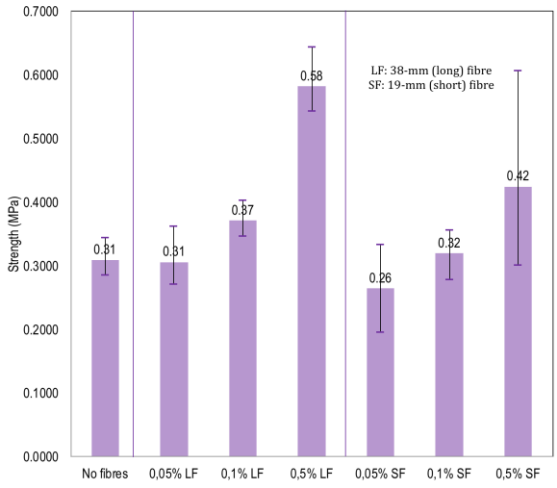

(c)

Figure 3.12. Tensile strength at (a) -5°C, (b) 5°C, (c) 20°C

It can be observed in **Figure *3.12*** that, in all cases, the highest tensile strength is given by the mix with the highest amount of fibre in its structure (0.5%). An interesting phenomenon can be seen when 0.1% dosage of fibres were added to mortar resulting in significant improvement at the lowest temperature (-5°C) than that of one at the higher temperature. Thus, the reinforcement with synthetic fibres leads to improved low-temperature cracking characteristics under monotonic fracture conditions. Another remark is that the different amount of fibres, after a

certain amount, does not give a dramatic impact at the lowest temperature. An explanation for this phenomenon is that while the increase of fibre dosage in the specimen will enhance the force transfer capacity between the fibre, the weakest link inside the sample is the adhesive bonding that is governing in the interface of fibre-matrix. On the other hand, the outcome of the incorporation of fibre into the specimen is more evident at high temperature. The phenomenon comes in account of the failure mode related to chapter 2, in which the adhesion of fibre-matrix is stronger than the cohesive strength of the mortar itself. Thus, the transmission of force through the fibre, whose stiffness is way higher than the matrix, is enhanced by a higher fraction of fibre. In general, the tensile strength increased with the addition of synthetic fibres into asphalt mortar, an observation also seen by incorporating other types of fibres in the past. [12]

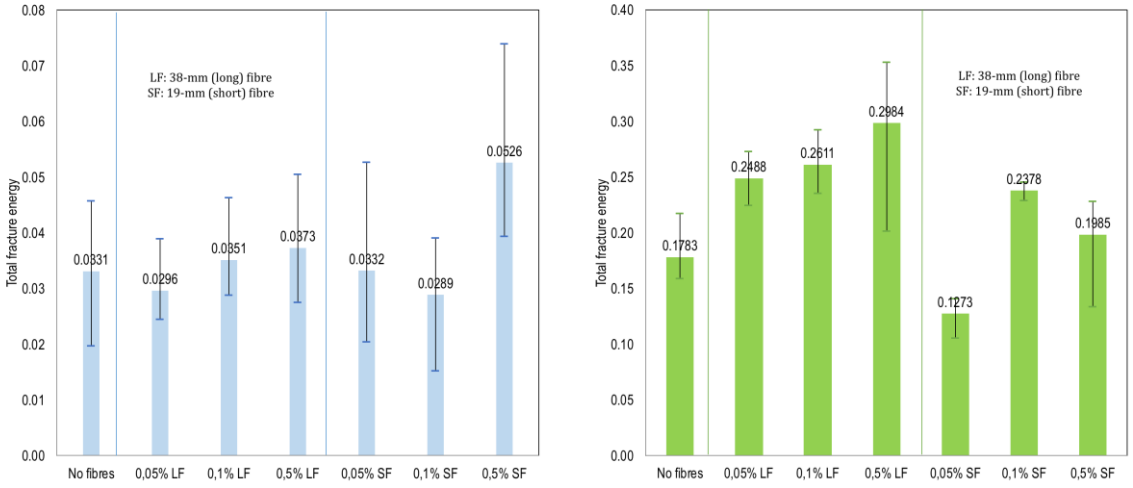

(a) (b)

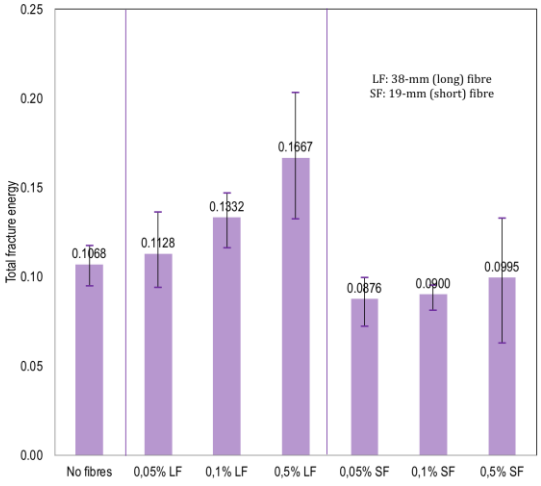

(c)

Figure 3.13. Fracture energy at (a) -5ºC, (b) 5ºC, (c) 20ºC

Since higher total energy means the higher capacity of a material to absorb any applied energy until its failure point, the high values of energy are desirable. The increase of energy required to cause failure to the material, such as tensile fracture, is corresponding to the total force needed to crush the material as well as the total elongation under loading. The results shown in **Figure *3.13*** indicate that the increase of the dosage of fibre included in a specimen improve the performance in terms of the amount of energy required to fracture the specimen under monotonic tensile loading. Regardless, there are several results that disagree with the premise. The difference can be elaborated that the presence of the fibre must be able to transfer a significant force through its body. If there is an insufficient amount of fibre at any location to transfer the force, the load will be then transferred to the matrix via adhesive bonding reaction. Since the interfacial zone has become the potential weak spot in a test in low temperature, this condition then potentially causes the failure to occur faster at the specimen, which then reduces the total amount of energy.

Furthermore, whereas the behaviour of the asphalt mortar with 19mm fibre (short fibre) is highly similar to that of the mortar sample using 38-mm fibre, it is evident that the behaviour shown in the mixture with the dosage of 0.1% of 38-mm fibre is comparable to that of 0.5% of 19-mm fibre in almost every testing property. This is, in fact, coming from a lower contact area available within the 19-mm fibre and the matrix relative to the 38-mm one, thus limiting the ability to transfer the force.

The second part of this research is carried out by performing the cyclic test with the force level at 35% of the peak force obtained from the monotonic test. The result of the tests is shown in **Figure *3.14***.

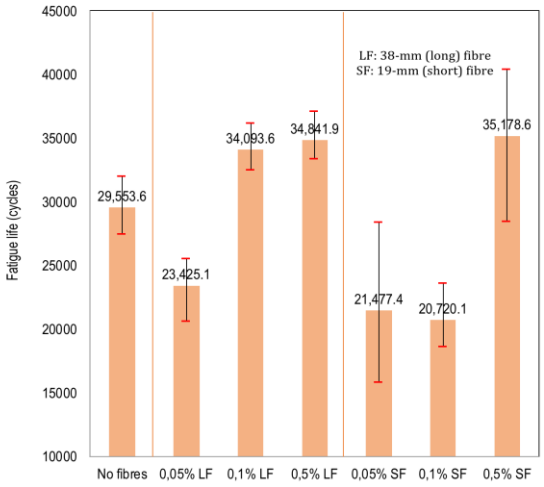

Figure 3.14. Fatigue life of mortar sample with different fibre content subjected to cyclic loading at 5°C

Several conclusions can be drawn upon this test. Firstly, it is evident that the highest dosage of the 38-mm fibre which is used does not give any significant contribution to the fatigue life, as it is close to the one of 0.1% fibre content. Moreover, the dosage of 0.05% gives the worst behaviour of all other recipes. The test results of the standard fibre (19-mm) show a bit contradiction to the 38mm one. While the amount of the fibre remains proportionally related to the fatigue life, the dosage of 0.1% behaves similarly to the dosage 0.05% with a high increment is exhibited by mixture with the dosage of 0.5%. The phenomena of a certain amount of fibre generate a worse fatigue capacity than the control mixture can be understood by the load transfer mechanism. Since it is already known that at low temperature the bonding strength between mortar-fibre is lower than the strength of the stiff mortar itself, sufficient amount of fibre is necessary so that the load can be transferred through the fibre connection and sustain the fatigue life of the sample. Otherwise, the existence of one single fibre can react as a "lubrication" agent the mortar, since the existence of the fibre could interfere the connection of other components and generate an imperfection.

Meanwhile, another research [23] has documented the same phenomenon, which was suspected as the effect of a high strain level. However, further research to examine the effect of strain level needs to be executed to achieve a better understanding.

It can be concluded then that a high dosage of 19-mm fibre is necessary to improve the fatigue life of a mortar specimen, while the use of the 38-mm fibre could reach an equivalent performance to the specimen, to which the 19-mm is incorporated, with a lower proportion of fibre necessary.

3.5 CONCLUSIONS AND RECOMMENDATIONS

Direct tension – monotonic loading test is able to locate the improvement brought by the synthetic fibre. In terms of peak stress, the effect is not so significant at low temperature as it is at high temperature, mainly caused by the fact that the adhesion of fibre-matrix is the weakest point in the specimen and only the transfer of loading between the fibre brings the positive effect, whereas the fibre is mainly responsible to the strength of the mix at high temperature, in which its adhesive bonding is stronger than the cohesive between the matrix itself. Both cases still show the increase of fibre content is directly proportional to the strength, nonetheless.

The total amount of fracture energy is associated with both stress and elongation of the sample under tension and means the total energy needed to damage the sample. Thus, a higher amount of energy is preferred. Generally, a higher fibre content will give the highest fracture energy. It is evident that the increase of the dosage of fibre is proportional to the increase in the amount of fracture energy, indicating better performance. Meanwhile, the addition of 19-mm fibre gives the equivalent trend as the 38-mm fibre, with a certain reduction in the values. The difference occurs

as the longer fibre has a higher contact area than the shorter one that provides a better force transfer.

Cyclic loading tension test is used to observe the fatigue life of an asphaltic mortar, specifically to identify the effect of the fibre added to the mix. It is found out that the increase of the dosage is able to extend fatigue life, with quite different behaviour is shown in the mix with longer to the shorter fibre. While the highest fatigue life (which is equivalent) is shown in both cases by the dosage of 0.5% fibre, the value is somehow comparable to the mix with the dosage of 0.1% of longer fibre; while the dosage of 0.05% and 0.1% of shorter fibre behave worse than the control mix.

Both monotonic and cyclic loading tension experiments conclude that the addition of 38-mm fibre with the dosage of 0.1% of mortar weight generates an equivalent performance to the mix with the dosage of 0.5% of 19-mm fibre. Therefore, it is presumed that the longer synthetic fibres could assist in reducing the number of fibres demanded in the production phase for reinforcing the asphaltic materials within the equivalent desired results.

4

Chapter Four: Fibre Reinforced Asphalt Concrete (FRAC)

4.1. INTRODUCTION

One of the major distresses in a pavement structure is cracking due to thermal and loading effect. A thorough examination is therefore necessary in order to recognise the mechanism of a crack, which is strongly related to the tensile strength of the mixture [44]. One of the most widely used methods to evaluate cracking of asphalt mixes is the Indirect Tension Test (ITT). However, this test shows several flaws regarding the risk of initiating a permanent deformation below the loading strip as well as the stress distribution at the centre of the specimen. A combination of tension-compression stress will occur simultaneously, and if the former is less than three times the latter, such a compressive failure will arise [45]. This test also encounters a problem in describing the fracture mechanics of a material that is vital in terms of addressing crack initiation and propagation in the material [46]. A semi-circular bending (SCB) test has then become a promising method to characterize the tensile strength and fracture energy of asphalt concrete. SCB test has been applied in pavement engineering field by several researches using different framework. Van de Ven [45] applied this test with aim of defining the tensile strength of a material in 1997, followed by Molenaar [47] and later Huang et al. [44] who were able to obtain the ratio of tensile strength of a SCB and ITT test material (tensile strength of SCB specimen is approximately 3.8 times higher than that of ITT sample). Another research by Molenaar et al [48] performed a finite element analysis to simulate the crack propagation, which initiates from the bottom fibre in the middle span of the sample (**Figure *4.1***). The graphs can be translated in following way. As the displacement due to the loading in top fibre goes higher, crack will start propagating from the bottom fibre where the tensile stress is at the highest level.

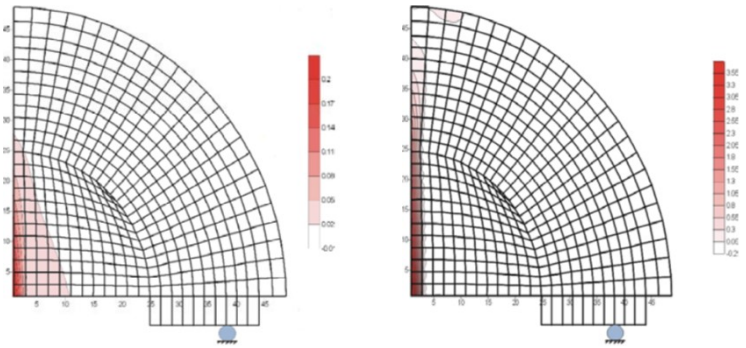

Figure 4.1. Crack propagation due to tensile loading modelled by Molenaar et al *[48]* at (left) t=2100 and (right) t=10500

The same paper compared the crack severity shown in **Figure *4.1*** with the crack severity due to the compressive effect, shown in **Figure *4.2***. It is clearly seen that the crack propagation at the specimen subjected to tensile loading is more severe than the compressive loading, thus also proving the role of cracking due to tensile force as the dominant failure mode at a SCB specimen. This makes the SCB test to be a better option than the ITT test.

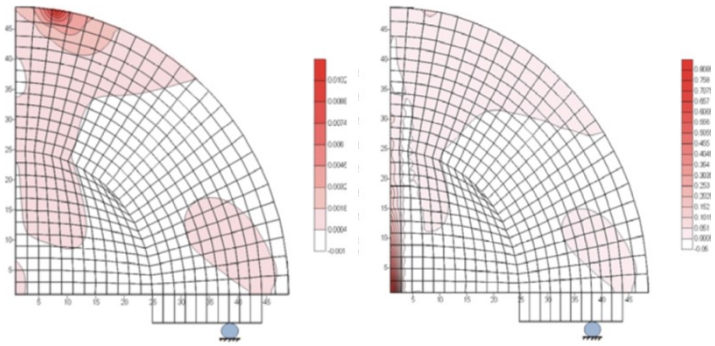

Figure 4.2. Crack propagation due to compressive loading modelled by Molenaar et al *[48]* at (left) t=2100 and (right) t=10500

Research conducted by Krans et al in 1996 [49] pointed towards fatigue capacity of of asphalt mixes. Another research by Li [46] suggested the possibility to define the fracture resistance of a bituminous specimen by means of this test, using different loading rate and different type of material. Furthermore, Li [46] and Nsengiyumva [50] have been able to investigate the effect of different parameters (notch depth, specimen thickness, test temperature and loading rate) to both tensile strength and fracture energy of the material. Evidently, higher notch depth decreases both tensile strength and fracture resistance, while the influence of specimen thickness is inversely proportional to both criteria. Furthermore, the effect of testing temperature is directly proportional to fracture energy and inversed to the peak strength. A higher loading rate is shown to increase the peak force and decrease fracture energy; however, it has only a small impact on the fracture energy at the lower temperature. It can be explained as the material gets stiffer at the

lower temperature and hence is less loading rate-dependant. The application of this test is then accompanied by a European standard (NEN-EN 12697-44) as well as American standard (AASHTO TP 105-13). Therefore, this research now adapts the norm to examine the effect of the aramid-polyolefin fibre to the tensile capacity as well as fracture resistance of a warm asphalt mix specimen.

4.2. METHOD AND PREPARATION

The type of asphalt concrete selected to be studied herein is as standard DAC-16 mix with the specification shown in **Table *4.1***. Moreover, there are two different fibre contents (0.05% and 0.5% of total specimen weight) and two different fibre lengths (19-mm and 38-mm) to be used. In order to study the effect of fibre length on the warm mix performance, several specimens with the inclusion of 38-mm fibre with the proportion of 0.1% are also investigated in this research.

First of all, the specific gravity of the aggregates needs to be examined. It is done by doing the test, with the result is shown in **Table 4.2**. The calculated specimen maximum density is 2484.4 kg/m^3 with expected void ratio of 7%.

Table 4.1. Fraction percentage of a semi-circular bending specimen (DAC-16)

Sieve Size [mm]	**Cumulative of agg. Passing [%]**		
	Lower limit	***Mix Composition***	*Upper limit*
22.00	100.00	**100.00**	100.00
16.00	94.00	**97.80**	100.00
11.20	75.00	**86.00**	95.00
8.00		**75.90**	
5.60	45.00	**59.20**	70.00
2.00	37.00	**38.10**	43.00
0.50		**16.00**	
0.18		**8.20**	
0.063	5.84	**6.10**	7.34
Bitumen (50/70)		***5.00***	

Table 4.2. Density of each aggregate fraction

	Agg 11-16	**Agg 8-11**	**Agg 5-8**	**Agg 2-5**
Dry weight (gr)	993.6	997	997.3	998
SSD weight in air (gr)	996.71	1001.7	1003.52	1002.5
SSD weight under water (gr)	628	631.45	631.02	631.46
Apparent specific gravity (Gsa)	2.718	2.727	2.723	2.723

The preparation of the specimens is made by using gyratory compactor based on the norm NEN-EN 12697-31. Firstly, the mould for compacting the gyratory sample has to be prepared for at least 2 hours prior to its use within the test temperature. The already mixed material should be poured into the mould afterwards by using a funnel. The mould is brought out of the compactor and cooling down for around 10 minutes, and then the specimen could be de-moulded. Four SCB samples could be cut from one gyratory sample. The geometry of the cylindrical gyratory sample is 150mm by height and 150mm by diameter(D). The height (W) of an SCB-sample cut from the gyrator sample is 50mm.

A notch is created at the centre with a depth of (12.5±3.5) mm and width of (3.0±0.1) mm. The width of the notch, which is the modification from the Eurocode, is approximately ten times larger than the norm. This dimension is based on the capacity of the production system provided in TU Delft, and the same approach is used in the research conducted by Elseifi et al. [51] with the result of the crack propagating exactly at the centre. The shape of an SCB shape is described by **Figure *4.3***

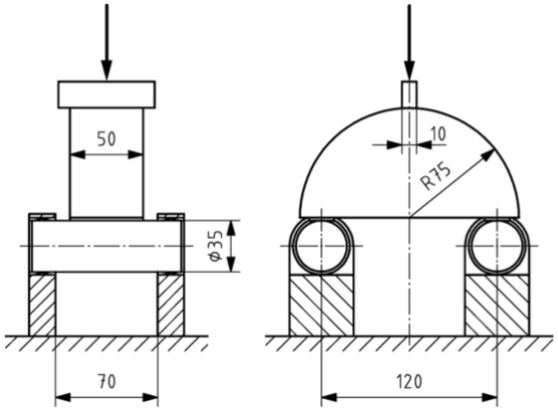

Figure 4.3. Sketch of a semi-circular bending test specimen specification

A compression load is transferred from the load cell to a loading metal strip placed on top of the specimen, with the purpose to evenly distribute the force over the total thickness. The external force from top exert two reaction forces from the support at the bottom part, within the distance

of 0.8 times the length of the specimen. A simply supported beam with a point load is best at resembling the testing condition, meaning that the highest bending (and stress) occurs in the middle of the span, with the highest tensile stress occurs mainly at the bottom fibre of the middle span. As the result, crack will initiate from the position.

The tested specimen is pre-conditioned in the test chamber at (0±1)°C for at least 4 hours, while the others have to be kept on a flat surface in a climate chamber. Then the test is carried out at a displacement rate of 5 mm/min. The test result can be considered as valid if only the crack ends in the zone of ±15 mm from the centre of the loading strip, see **Figure *4.4***.

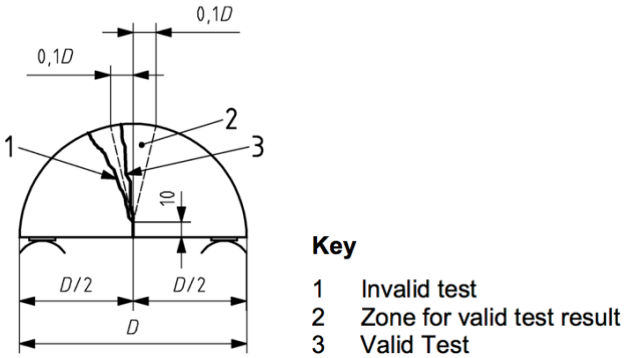

(b)

Figure 4.4. Failure location criterion

Several results could be produced out of the force-displacement curve, by means of following equations.

Tensile strength ($\sigma_{max,i}$). The strength of material is computed using following expression.

$$\sigma_{max,i} = \frac{4.263 \cdot F_{max,i}}{D_i \cdot t_i} \quad N/mm^2 \qquad \textbf{4.1}$$

where: $F_{max,i}$ is max. force of specimen number i in N, D_i is diameter of specimen number i in mm, and t_i is the thickness of specimen number i in mm.

The constant 4.263 is derived by the research conducted by Van de Ven et al. [45] by means of a 3D finite element analysis using the assumption of support span at 80% of the sample length or diameter (D).

Fracture toughness (K_{Ic}). The toughness of the material, which describes ability of a material to resist fracture, can be calculated by following equation.

$$K_{Ic,i} = \sigma_{max,i} \cdot f\left(\frac{a_i}{W_i}\right) {}^{N}/_{mm^{1.5}} \quad \textbf{4.2}$$

where: W_i is height of specimen i in mm, a_i is depth of the notch of specimen i in mm, $\sigma_{max,i}$ is stress at failure of specimen i in N/mm2, and $f\left(\frac{a_i}{W_i}\right)$ is the geometry factor of specimen i which is dimensionless and should be rounded to three digits. The geometry factor is determined by following expression.

For 9 mm < a_i < 11 mm and 70 mm < W_i < 75 mm, then $f\left(\frac{a_i}{W_i}\right)$ = 5.956, otherwise:

$$f\left(\frac{a_i}{W_i}\right) = -4.9965 + 155.58\left(\frac{a_i}{W_i}\right) - 799.94\left(\frac{a_i}{W_i}\right)^2 + 2141.9\left(\frac{a_i}{W_i}\right)^3 - 2709.1\left(\frac{a_i}{W_i}\right)^4 + 1398.6\left(\frac{a_i}{W_i}\right)^5 \quad \textbf{4.3}$$

Strain ($\boldsymbol{\varepsilon_{max,i}}$). The strain that is obtained here is the strain at the maximum force, which is computed as follows.

$$\varepsilon_{max,i} = \frac{\Delta W_i}{W_i} \cdot 100\% \quad \textbf{4.4}$$

where: ΔW_i is the vertical displacement of sample i in mm, and $W_i$is the height of specimen i in mm.

Fracture energy (Gf). It is calculated by the division of the fracture work and ligament area.

$$G_f = \frac{W_f}{A_{lig}} \quad \textbf{4.5}$$

where: W_f (fracture work) is defined as the area of a force-displacement curve and A_{lig} is the ligament area, calculated as (radius of specimen – notch length) * specimen thickness

4.3. RESULTS AND DISCUSSION

The result from the test is the same as it is from direct tension test, which is a series of data set of force-displacement. A fitting curve is then developed from the data with the purpose to be able later to obtain the area under the force-displacement curve, recognised as the total fracture energy. There are three different categories that will be discussed within this section, as follows.

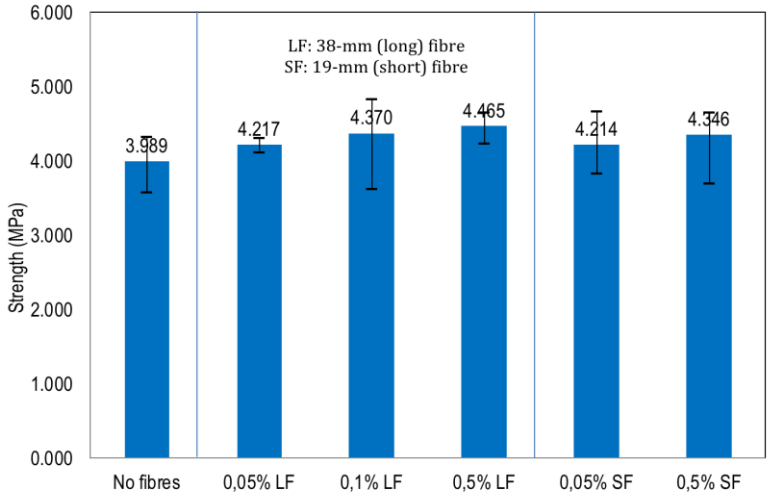

(a)

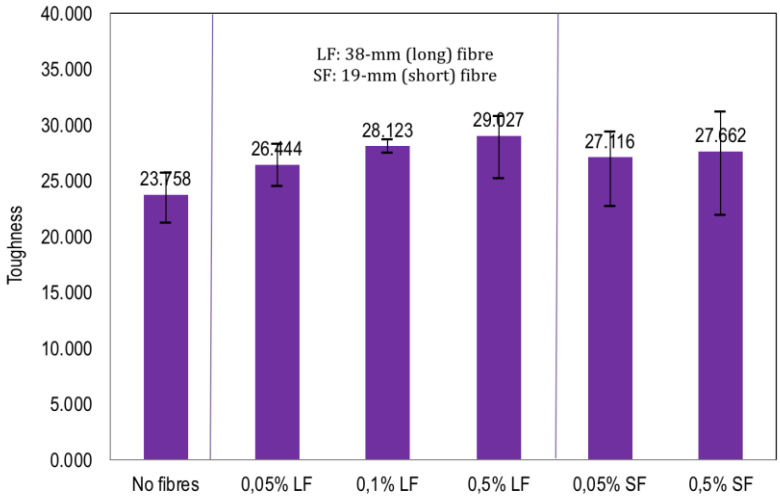

(b)

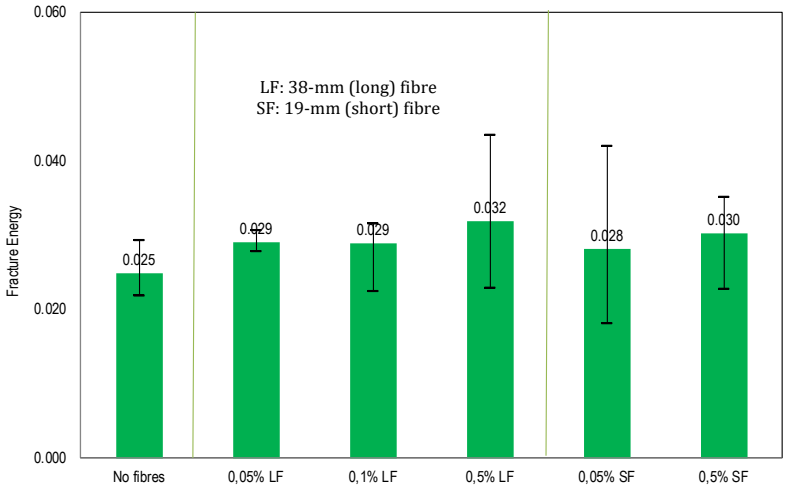

(c)

Figure 4.5. (a) Peak stress, (b) fracture toughness and (c) total fracture energy at 0°C

Firstly, **Figure *4.5*** (a) demonstrates that the addition of synthetic fibres provides a reinforcing effect to asphalt mix at low temperature. It can also be seen that the addition of 0.1% by weight of longer fibres (38-mm) could generate an equivalent performance to the 0.5% of shorter one (19-mm), as it is also prescribed from direct tension test result. Such a possible explanation is that a higher stiffness formed by the bonding of aggregate-matrix that contributes to the high strength of the specimen, whereas the inclusion of fibre induces adhesion of fibre-matrix which, at low temperature, becomes the weak spot of the sample. However, the ability to transfer the force between the fibre enacts a reinforcing effect at low temperature, provided that the amount of fibre is sufficient, hence making the strength of the fibre-reinforced asphalt concrete (FRAC) with long fibre is higher than the short one.

The term toughness refers to the ability of a subject to carry loading until its breaking point. While toughness is typically associated to the total amount of energy needed to fracture a material, the toughness in Eurocode is related to the strength and the shape factor (i.e., notch depth) herein. As depicted from **Figure *4.5*** (b), the toughness is enhanced proportionally to the dosage of the fibre, with a more significant impact brought by the longer fibre due to the same explanation as of the behaviour of strength.

Additionally, the total fracture energy (**Figure *4.5***c), which is the area under a stress-strain curve, illustrates the amount of work needed to bring material to its failure state. The difference between this approach and the "toughness" described by the Eurocode is that this method does the calculation in respect to the strength and the elongation of the material from the test result, whereas the approach from Eurocode does not consider the elongation, but takes into account the effect of notch depth into the calculation. This method then can be considered as a conventional one. The trend, however, remains the same, as the higher proportion of fibre boost the amount of fracture energy, regardless of the fibre length.

Finally, the results may vary due to the distribution of the fibre in the specimen. By performing a SCB test and since failure is imposed to locate precisely at the mid-span, thanks to the notch, the results describe mainly the contribution of the fibre at the mid-span. It is then believed that the total impact is not given by fibre network, since the fibre should be widespread through the whole body of specimen. Thus, the results may vary due to the fibres distribution in the specimen. Another testing method which is able to activate the role of fibre inside the whole specimen, such as a four-point bending test, is suggested for the AC mixture scale. Furthermore, the impact of the fibre on fatigue life of the AC specimen should also be examined, since the presence of fibre is proven to be able to increase the fatigue life of AC mix.

4.4. CONCLUSIONS

A semi-circular bending test is meant to examine the behaviour of a dense asphalt concrete more comprehensively. In this case, the contribution of the synthetic fibre to tension performance of studied mix is demonstrated. The results indicate that the inclusion of fibre increases the performance of the AC mixture. Tensile strength as the first criterion is enhanced proportionally by increasing fibre dosage. However, the difference is not distinctive, ultimately between 0.1% and 0.5% dosage of 38-mm fibre. It is also found out that the reinforcing effect brought by 38mm-fibre is higher than the 19mm one. Secondly, toughness also shows a prominent trend. Finally, fracture energy gives the similar tendency as the overall results. A conclusion can be drawn based on the mentioned criteria that the overall mechanical response of 0.1% w/w of 38mm- fibre is comparable to that with 0.5% w/w of 19mm-fibre, as also found out in the previous phase.

5

Conclusion and Suggestion

The findings of this research elucidated that implementing the aramid-polyolefin synthetic fibre into warm-mix asphalt material by using multi-scales experimental technologies can assist on understanding the insight into the function mechanism of reinforced warm-mix asphalt pavement and hence tailoring the system with optimization of the usage of reinforcement dosages and fibre length.

This research has been able to perform a thorough examination on the beneficial effect of the incorporation of synthetic fibre, as the outcome generally shows that the increase of fibre length, as well as its dosage, generate a higher degree of improvement to any tested specimen in terms of tensile strength and fracture energy. The research highlights two phenomena: firstly, the reinforcing effect is more evident at high temperature. This is possible since the adhesion of fibre and the matrix is significantly stronger than the strength of the mortar itself. Secondly, the performance of the asphaltic specimen added with a dosage of 0.5% 19-mm length fibre is equivalent to the specimen with the dosage of 0.1% 38-mm length fibre. This occurs due to a higher capacity to transfer of load that is enabled by a higher length of the fibre. Therefore, it is suggested to incorporate the dosage of 0.1% of the 38-mm fibre to a warm mix asphalt.

To sum up, this thesis project has been able to extend the knowledge on the mechanism of synthetic fibre reinforcement inside an asphaltic mixture, as well as to give a recommendation of the desired fibre length and dosage to be used in the regarded composition of warm asphalt mix. The findings could become a comprehensive reference for the asphalt pavement production using the type of asphalt mix and synthetic fibre system.

There are several suggestions for improvement for each phase of this research. Firstly, the range of the testing temperature for the pull-out test should be expanded in order to study different failure mechanisms that could be governing to the specimen response. Hence, a more proper testing apparatus that could provide a better clamping, as well as a higher loading capacity, is necessary to actualise the purpose.

Secondly, direct tension test could study further the effect of the degree of the improvement brought by the synthetic fibre to a mortar specimen when subjected to different tensile monotonic

loading speeds. Furthermore, the effect of different loading frequency can be taken into account for the cyclic loading test to get a better understanding towards the suitability of the inclusion of fibre to a road pavement construction with different traffic conditions.

Finally, the study of the effect of the addition of synthetic fibre to an asphaltic mixture using semi-circular bending test could be extended by using a cyclic tensile loading to get the response regarding fatigue capacity. Furthermore, since the critical location of the semi-circular bending specimen is limited at the centre part, then another testing method (such as a four-point bending test) needs to be executed so that the contribution of the fibre in the entire section of the specimen can be examined.

Bibliography

[1] „TRB Circular E-C165: Alternative Binders for Sustainable Asphalt Pavements," Transportation Research Board of the National Academies, Washington, D.C., 2002.

[2] „TRB Circular E-C186: Enhancing Durability of Asphalt Pavements.," Transportation Research Board of the National Academies, Washington, D.C., 2014.

[3] R. Mcdaniel, „Fiber Additives in Asphalt Mixtures," *NCHRP SYNTHESIS 475,* 2015.

[4] M. Zaumanis en J. Smirnovs, „Analysis of Possibilities for Use of Warm Mix Asphalt in Latvia," in *Civil Engineering '11 - 3rd International Scientific Conference*, 2011.

[5] M. Zaumanis, Asphalt is Going Green, LAP LAMBERT Academic Publishing GmbH & Co. KG, 2011.

[6] R. West, C. Rodezno, G. Julian en B. Prowell, „Field Performance of Warm Mix Asphalt Technologies," TRANSPORTATION RESEARCH BOARD, 2014.

[7] J. D'Angelo, E. Harm, J. Bartoszek, G. Baumgardner, M. Corrigan, J. Cowsert, T. Harman, M. Jamshidi, W. Jones, D. Newcomb, B. Prowell, R. Sines en B. Yeaton, „Warm-mix asphalt: European practice," US Departmentt of transportation, 2008.

[8] B. Prowell en G. Hurley, „Warm-Mix Asphalt: Best Practices," *Quality Improvement Publication 125, 3rd Edition.,* 2012.

[9] A. Chowdhury en J. Button, „A review of warm mix asphalt," Texas Transportation Institute. Texas A&M University System., 2008.

[10] J. Serfass en J. Samanos, „Fiber-modified asphalt concrete characteristics, applications and behavior," *Asphalt Paving Technology: Association of Asphalt Paving Technologists,* vol. 65, pp. 193-230, 1996.

[11] H. Busching, E. Elliott en N. Reyneveld, „A STATE-OF-THE-ART SURVEY OF REINFORCED ASPHALT PAVING," *Proceedings of the Annual Meeting of the Association of Asphalt Paving Technologists,* vol. 39, pp. 766-798, 1970.

[12] P. Apostolidis, „Experimental and Numerical Investigation of Induction Heating in Asphalt Mixes," Repository of TU Delft, Delft.

[13] B. Putnam, „Effects of Fiber Finish on the Performance of Asphalt Binders and Mastics," *Advances in Civil Engineering,* p. 11, 2011.

[14] J. McIntyre en P. Daniels, Textile terms and definitions, vol. 10, Manchester: The Textile Institute, 1991.

[15] M. Jassal en S. Ghosh, „Aramid fibres-An overview," *Indian Journal of Fibre and Textile Research,* vol. 27, nr. 3, pp. 290-306, 2002.

[16] T. Hutley en M. Ouederni, „Polyolefins—The History and Economic Impact," in *Polyolefin Compounds and Materials - Fundamentals and Industrial Applications*, Springer, Cham, 2016, pp. 13-50.

[17] Aramid Fiber of Poly Para-Phenylene Terephthalamide From The Netherlands, Washington, D.C.: U.S. International Trade Comission, 1994, pp. II-9.

[18] K. Chang, „Aramid Fibers," pp. 41-45, 2001.

[19] S. Van Der Zwaag, „Structure and properties of aramid fibres," in *Handbook of Textile Fibre Structure - Fundamentals and Manufactured Polymer Fibres*, vol. 1, Woodhead Publishing Limited, 2009, pp. 394-412.

[20] R. Mather, „The structure of polyolefin fibres," in *Handbook of Textile Fibre Structure - Fundamentals and Manufactured Polymer Fibres* , Woodhead Publishing Limited, 2009, pp. 276-304.

[21] D. Sauter, M. Taoufik en C. Boisson, „Polyolefins, a Success Story," *Polymers,* vol. 9, nr. 6, p. 185, 2017.

[22] S. Tapkin, „The effect of polypropylene fibers on asphalt performance," *Building and Environment,* vol. 43, 2008.

[23] K. Kaloush, W. Zeiada, K. Biligiri, M. Rodezno en J. Reed, „Evaluation of Fiber-Reinforced Asphalt Mixtures Using Advanced Material Characterization Tests," in *The First Pan American Geosynthetics Conference & Exhibition*, Cancun, 2008.

[24] J. Stempihar, M. Souliman en K. Kaloush, „Fiber-Reinforced Asphalt Concrete as Sustainable Paving Material for Airfields," *Journal of the Transportation Research Board,* nr. 2266, pp. 60-68, 2012.

[25] C. Ho, J. Shan, F. Wang, Y. Chen en A. Almonnieay, „Performance of Fiber-Reinforced Polymer Modifed Asphalt two-Year review in Northern arizona," *Journal of the Transportation Research Board,* nr. 2575, pp. 138-149, 2015.

[26] T. Takaikaew, P. Tepsriha, S. Horpibulsuk, M. Hoy, K. Kaloush en A. Arulrajah, „Performance of Fiber-Reinforced Asphalt Concretes with Various Asphalt Binders in Thailand," *Journal of Materials in Civil Engineering,* vol. 30, nr. 8, August 2018.

[27] DIBEC; TU Delft, „Influence of Forta Fibres on Dutch HMA and WMA," 2016.

[28] Fibremax Ltd, „Aramid Fiber," [Online]. Available: http://www.aramid.eu/advantages---disadvantages.html. [Geopend August 2018].

[29] C. Rieger, Micro-Fiber Cement Pullout Tests, Uniaxial Tensile Tests and Material Scaling, Zürich: ETH Zürich, 2010.

[30] I. Markovich, J. van Mier en J. Walraven, „Single fiber pullout from hybrid fiber reinforced concrete," 2001. [Online]. Available: https://repository.tudelft.nl/islandora/object/uuid:c9e570f1-09d8-4d7f-9b35-00be7173fc50/datastream/OBJ/download. [Geopend 5 7 2018].

[31] M. Sayed, Plant Fibre Reinforced Composites: Abaca fibres in concrete - Investigation on the possible application of Abaca fibre as reinforcement in concrete to create ductility, Delft: Delft University of Technology, 2014.

[32] P. Park, S. El-Tawil en A. Naaman, „Pull-out behavior of straight steel fibers from asphalt binder," *Construction and Building Materials,* vol. 144, pp. 125 - 137, 2017.

[33] S. Qian, H. Ma en J. Feng, „Fiber reinforcing effect on asphalt binder under low temperature," *Construction and Building Materials,* vol. 61, pp. 120-124, 2014.

[34] Anton Paar GmbH, „Anton-Paar.com," Anton Paar, [Online]. Available: https://www.anton-paar.com/corp-en/products/group/dynamic-mechanical-analysis/. [Geopend 14 09 2018].

[35] L. Mo, „DAMAGE DEVELOPMENT IN THE ADHESIVE ZONE AND MORTAR OF POROUS ASPHALT CONCRETE," Technische Universiteit Delft, Delft, 2009.

[36] C. Gao en W. Wu, „Using ESEM to analyze the microscopic property of basalt fiber reinforced asphalt concrete," *International Journal of Pavement Research and Technology,* 2018.

[37] P. Bolzan en G. Huber, „Direct Tension Test Experiments," Strategic Highway Research Program, Austin, 1993.

[38] S. Erkens en M. Poot, „The Uniaxial Tension Test - Asphalt Concrete Response (ACRe)," Delft University of Technology, Delft, 2001.

[39] N. Kringos, R. Khedoe, A. Scarpas en A. de Bondt, „A New Asphalt Concrete Moisture Susceptibility Test Methodology," in *Transportation Research Board 90th Annual Meeting*, Washington, D.C., 2011.

[40] B. Huang, G. Li en L. Mohammad, *Analytical modeling and experimental study of tensile strength of asphalt concrete composite at low temperatures,* pp. 705 - 714, 2003.

[41] G. Leegwater, A. Scarpas en S. Erkens, „Direct Tensile Test to Assess Healing in Asphalt," *Journal of the Transportation Research Board,* nr. 2574, pp. 124 - 130, 2016.

[42] C. B. Nielsen, „Microstructure of porous pavements-- Experimental procedures," Road Directorate, Danish Road Institute, Hedehusene, 2007.

[43] G. Liu, „Characterization and Identification of Bituminous Materials Modified with Montmorillonite Nanoclay," Delft University of Technology, Delft, 2011.

[44] B. Huang, X. Shu en Y. Tang, „COMPARISON OF SEMI-CIRCULAR BENDING AND INDIRECT TENSILE STRENGTH TESTS FOR HMA MIXTURES," *Advances in Pavement Engineering,* 2005.

[45] M. van de Ven, A. d. F. Smit en R. L. Krans, „POSSIBILITIES OF A SEMI-CIRCULAR BENDING TEST," *Transportation Research Board,* vol. II, pp. 939-950, 1997.

[46] X.-J. Li en M. Marasteanu, „Using Semi Circular Bending Test to Evaluate Low Temperature Fracture Resistance for Asphalt Concrete," *Experimental Mechanics,* 2009.

[47] A. Molenaar, A. Scarpas, X. Liu en S. Erkens, „Semi-Circular Bending Test: Simple But Useful?," in *Association of Asphalt Paving Technologists-Proceedings of the Technical Sessions*, 2002.

[48] J. Molenaar, X. Liu en A. Molenaar, „RESISTANCE TO CRACK-GROWTH AND FRACTURE OF ASPHALT MIXTURE," in *6th RILEM Symposium PTEBM'03*, Zurich, 2003.

[49] R. Krans, F. Tolman en M. Van de Ven, „Semi-Circular Bending Test: A Practical Crack Growth Test Using Asphalt Concrete Cores," in *Third International RILEM Conference*, Maastricht, 1996.

[50] G. Nsengiyumva, „Development of Semi-Circular Bending (SCB) Fracture Test for Bituminous Mixtures," Civil Engineering Theses, Dissertations, and Student Research; University of Nebraska - Lincoln, Nebraska, Lincoln, 2015.

[51] M. Elseifi, L. Mohammad., H. Ying en S. Cooper III, „Modeling and evaluation of the cracking resistance of asphalt mixtures using the semi-circular bending test at intermediate temperatures," in *Road Materials and Pavement Design*, Taylor and Francis, 2012, pp. 124-139.

A. APPENDIX A: Preliminary Project – DIBEC&TU Delft

The project was carried out in October 2016. It consisted of three standard tests, namely four-point bending test, triaxial test, and indirect tension test, shown in **Figure *A.1***. The purposes were to obtain the effect of the incorporation of synthetic fibre to stiffness and fatigue life, resistance to permanent deformation, and to susceptibility to moisture measured by tensile strength. **Table *A.1*** presents the final result of every examination.

(a)

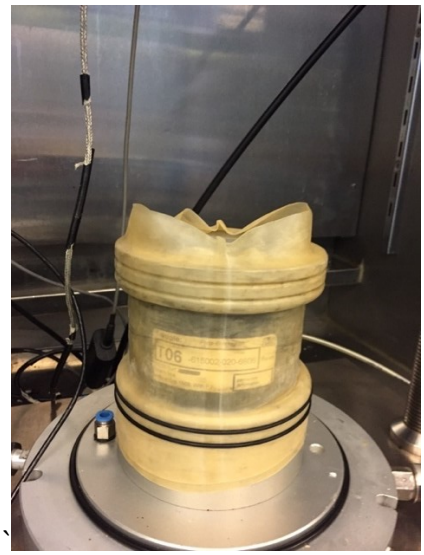

(b)

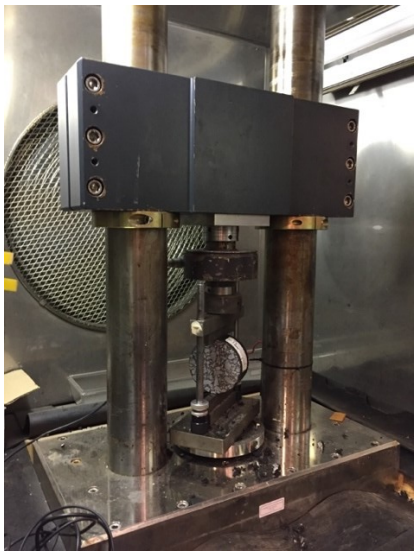

(c)

Figure A.1. The setup of (a) Four-point bending test, (b) triaxial test and (c) indirect tensile test

Table A.1. Final result of standard tests

		Without Fiber	**With Fiber**
Stiffness	Frequency (Hz)	Stiffness (Mpa)	Stiffness (Mpa)
	0.1	1535	1404
	0.5	2193	1809
	1	2869	2678
	2	3754	3521
	5	5181	4851
	8	5998	5712
	10	6411	6104
	20	7819	7416
	30	8552	8316
	0.1	1148	1059
Fatigue	Smix (Mpa)	7789	7493
	e6 (μm/m)	95.000	101.000
	log k1	16.477	15.477
	k2	-5.295	-4.731
	q = A0	37.940	35.640
	p = A1	-5.295	-4.731
	R2	0.977	0.983
	used strain	80/120/200	
water sensitivity	kmax wet (kN)	17.214	16.958
	kmax dry (kN)	18.140	18.485
	ITS wet (Mpa)	2.146	2.136
	ITS dry (Mpa)	2.269	2.305
	ITSR	94.6%	92.7%
Triaxial	A1 (%)	0.885	1.522
	B1 (%)	0.0003399	0.0002699
	fc (μm/m/cycle)	3.400	2.700
	A (%)	0.086	0.370
	B	0.399	0.237
	e1000, calc (%)	1.225	1.792

B. APPENDIX: Pullout Testing

The result of the tests conducted in MCR apparatus is presented in **Table *B.1***.

Table B.1. Final result of pull-out test

Fibre content	**Strength**			
	Sample 1	Sample 2	Sample 3	Average
0.2 mm/s	11.34	10.89	9.58	**10.6033**
0.1mm/s	7.8600	8.6300	7.16	**7.8833**
0.05mm/s	3.5600	4.1100	4.1300	**3.9333**
0.025 mm/s	2.7400	2.1200	2.7500	**2.5367**

Figure *B.1* illustrates all test results in curves.

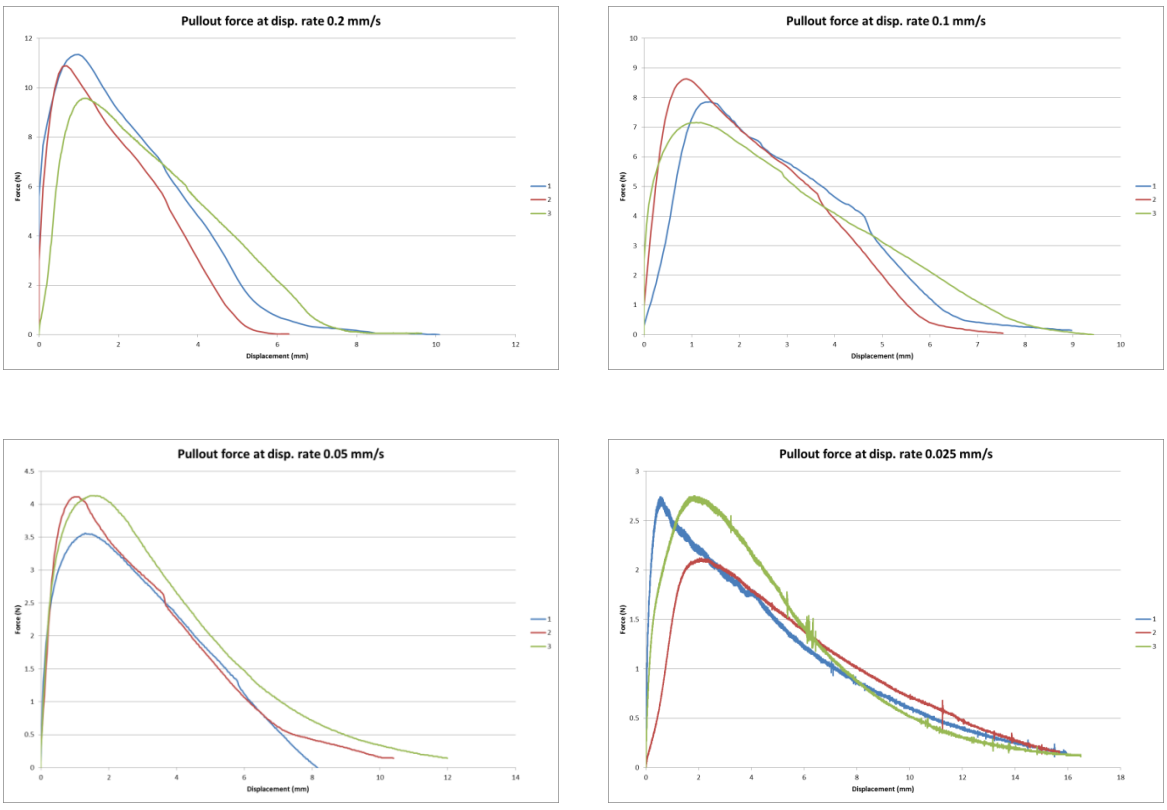

Figure B.1. Pull out force-displacement curves at different loading speed

C. APPENDIX: Direct Tension Test of Asphalt Mortar

The output of the direct tension test using a parabolic shape specimen is a series of time-displacement-force data; it can be used to construct a force-displacement curve, or can also be converted to a stress-strain series, provided that the only strain governing is the strain in the vertical direction. The result can then be uploaded to MATLAB to produce a probe curve followed with an equation (**Figure *C.1***), which will be useful primarily to calculate the total fracture energy.

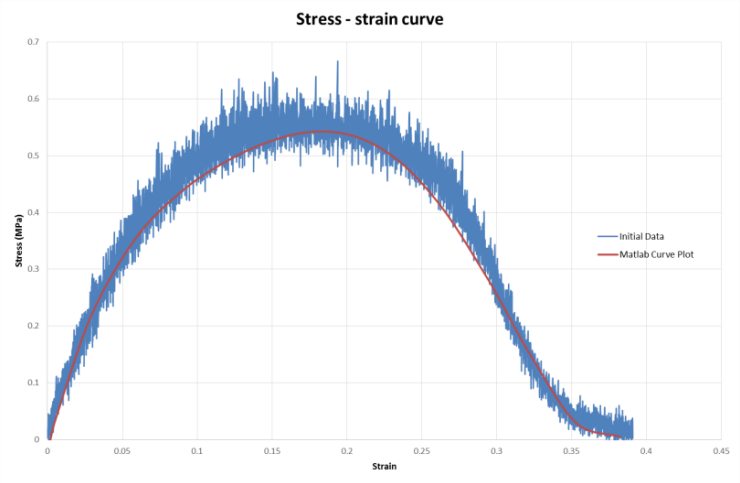

Figure C.1. Typical stress-strain curve vs plotting curve result from MATLAB

The red line is the fitting curve based on the data. The results and recapitulation are shown in **Figure *C.2*** and **Table *C.1*** to **Table *C.3***, respectively.

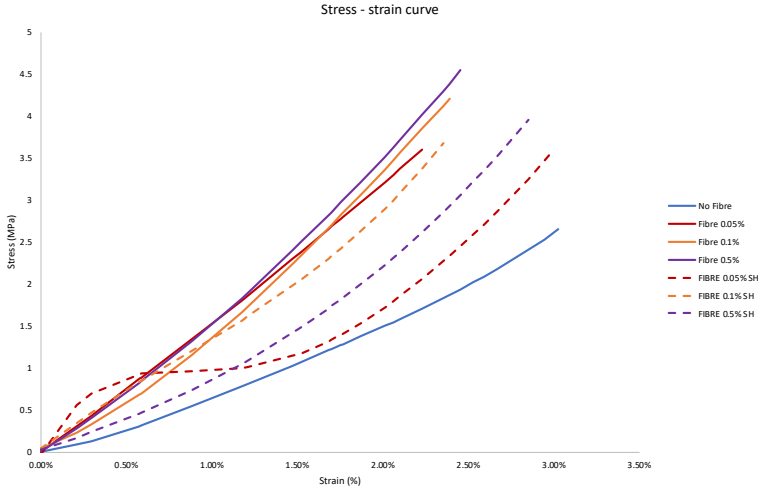

(a)

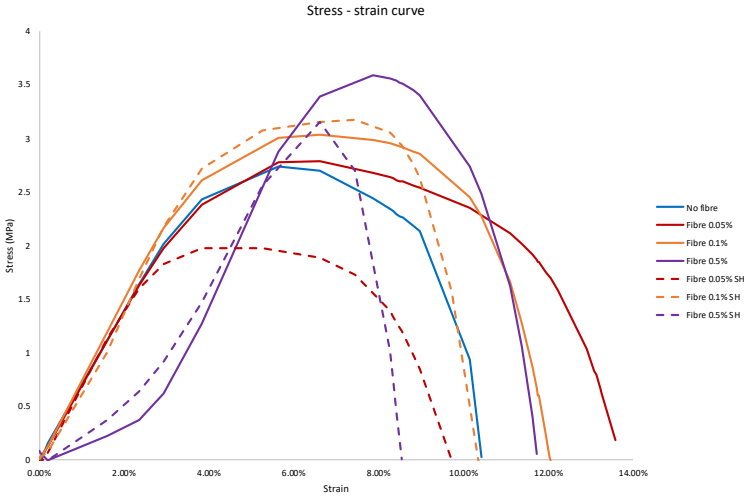

(b)

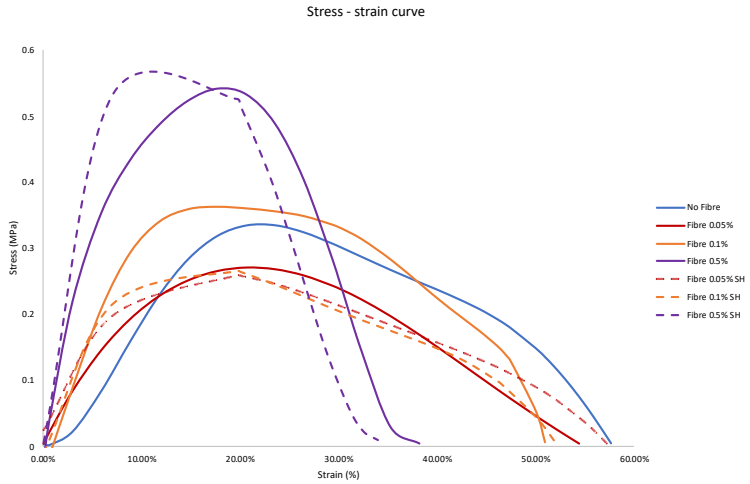

(c)

Figure C.2. Stress strain curves at (a) -5°C, (b) 5°C and (c) 20°C

Table C.1. Monotonic test result at -5°C

Fibre content	Strength			Energy	
		Average	R^2		Average
No fibre	2.7950	2.5059	0.9986	0.0456	0.0331
	2.6535		0.9956	0.0341	
	2.0692		0.9962	0.0196	
Fibre 0.05%	3.5984	3.0320	0.9988	0.0388	0.0296
	2.7559		0.9657	0.0244	
	2.7417		0.9566	0.0257	
Fibre 0.05% - 19mm	2.5764	3.9703	0.9943	0.0203	0.0332
	5.1527		0.9935	0.0268	
	4.1818		0.9919	0.0526	
Fibre 0.1%	4.2010	2.9281	0.9974	0.0462	0.0351
	2.3669		0.9982	0.0305	
	2.2163		0.9973	0.0287	
Fibre 0.1% - 19mm	2.3032	3.5568	0.9921	1.51E-02	0.0289
	3.7250		0.991	0.0327	
	4.6423		0.9975	0.0389	
Fibre 0.5%	3.7788	4.1155	0.9982	0.0274	0.0373
	4.0235		0.9944	0.0342	
	4.5441		0.9944	0.0503	
Fibre 0.5% - 19mm	3.6769	4.1129	0.9963	0.0393	0.0526
	4.7123		0.9946	0.0738	
	3.9496		0.9948	0.0447	

Table C.2. Monotonic test result at 5°C

Fibre content	Strength			Energy		Ductility	
		Average	R^2		Average		Average
No fibre	2.7650	2.7215	0.9959	0.2163	0.1783	0.044324	0.0362
	2.6535		0.992	0.1602		0.029297	
	2.746		0.975	0.1584		0.035	
Fibre 0.05%	2.7850	2.7455	0.9877	0.2722	0.2488	0.055615	0.0605
	2.7001		0.9901	0.2503		0.063176	
	2.7515		0.9882	0.224		0.062615	
Fibre 0.05% - 19mm	1.9924	2.4864	0.9835	0.1399	0.1273	0.05329	0.0374
	2.6927		0.9933	0.1375		0.03438	
	2.7742		0.9882	0.1044		0.02463	
Fibre 0.1%	3.1827	3.1949	0.9968	0.2919	0.2611	0.050294	0.0577
	3.0352		0.9918	0.2344		0.054235	
	3.3668		0.9845	0.257		0.068647	
Fibre 0.1% - 19mm	2.7135	3.0485	0.9833	0.2399	0.2378	0.062885	0.0483
	3.2567		0.9874	0.2451		0.05145	
	3.1754		0.9842	0.2285		0.03053	
Fibre 0.5%	3.6088	3.6596	0.9916	0.3524	0.2984	0.011294	0.0279
	3.8104		0.9953	0.201		0.03784	
	3.5595		0.9972	0.3418		0.034693	
Fibre 0.5% - 19mm	3.3838	3.2670	0.9916	0.2353	0.1985	0.040566	0.0332
	3.1574		0.9914	0.1325		0.01945	
	3.2597		0.9933	0.2276		0.039596	

Table C.3. Monotonic test result at 20°C

Fibre content	Strength			Energy		Ductility	
		Average	R^2		Average		Average
No fibre	0.34488	0.308863	0.9511	0.1174	0.106833	0.3459	0.405779
	0.29569		0.9627	0.1085		0.4573	
	0.28602		0.9379	0.0946		0.4141	
Fibre 0.05%	0.3626	0.306003	0.9572	0.1362	0.1128	0.4124	0.388053
	0.28466		0.9539	0.1086		0.4176	
	0.27075		0.9572	0.0936		0.3341	
Fibre 0.05% - 19mm	0.2628	0.264233	0.9301	0.0994	0.0876	0.4065	0.313533
	0.19623		0.8378	0.0719		0.3086	
	0.33367		0.8925	0.0915		0.2255	
Fibre 0.1%	0.36339	0.370847	0.9774	0.1369	0.133167	0.3391	0.355586
	0.40273		0.9676	0.1161		0.3100	
	0.34642		0.9305	0.1465		0.4176	
Fibre 0.1% - 19mm	0.27797	0.319343	0.9774	0.0951	0.090033	0.3720	0.313833
	0.3233		0.8764	0.0939		0.3560	
	0.35676		0.8764	0.0811		0.2135	
Fibre 0.5%	0.54387	0.58195	0.9803	0.1323	0.166667	0.2968	0.25941
	0.64383		0.986	0.1648		0.2791	
	0.55815		0.9624	0.2029		0.2024	
Fibre 0.5% - 19mm	0.60661	0.42434	0.976	0.1325	0.099533	0.2050	0.194667
	0.36532		0.9517	0.1036		0.2620	
	0.30109		0.9148	0.0625		0.1170	

Fatigue test is using a cyclic loading that is developed based on a loading frequency of 5Hz with the applied force 35% of the maximum force obtained from the monotonic test. Fatigue life here is defined as the very last cycle before being split. A typical fatigue curve for this test is shown in **Figure *C.3***, while **Table *C.4*** presents the complete results.

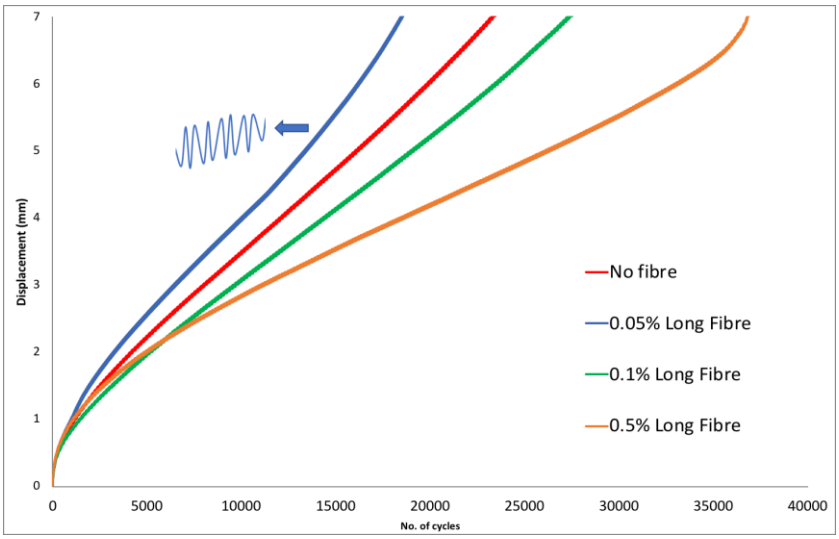

(a)

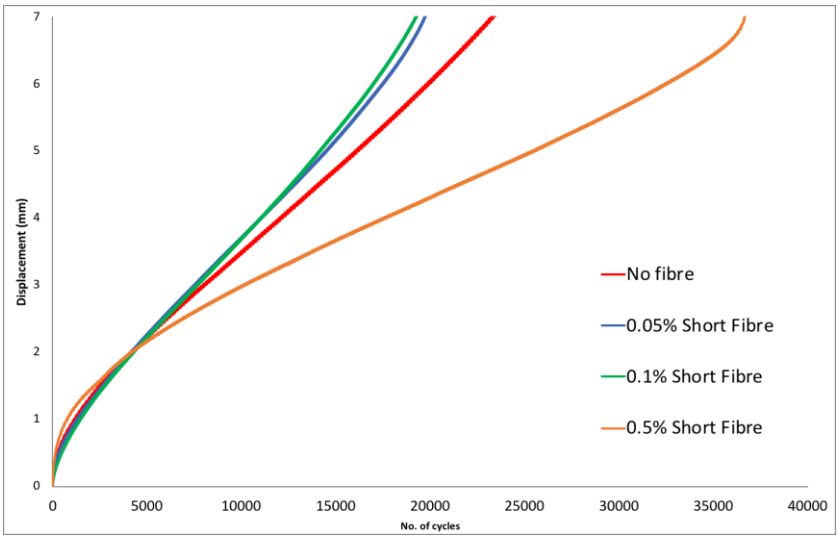

(b)

Figure C.3. Typical fatigue curve from cyclic loading test result of (a) control mix vs mix of long fibre and (b) control mix vs mix of short fibre

Table C.4. Cyclic loading test result

Fibre content	N (fatigue life in cycles)			
	Sample 1	**Sample 2**	**Sample 3**	**Average**
No fibre	29288.6	31938.6	27433.6	**29553.6000**
Fibre 0.05%	20591.8	25521.8	24161.8	**23425.1333**
Fibre 0.05% - 19mm	15781.8	20281.8	28368.6	**21477.4000**
Fibre 0.1%	33643.6	32478.6	36158.6	**34093.6000**
Fibre 0.1% - 19mm	18561.8	23546.8	20051.8	**20720.1333**
Fibre 0.5%	37068.6	33313.6	34143.6	**34841.9333**
Fibre 0.5% - 19mm	28413.6	36728.6	40393.6	**35178.6000**

D. APPENDIX: Semi-circular Bending Testing

An SCB test generates a data series consisting of force and displacement, which are then uploaded to MATLAB to develop a fitting curve, with the exact same method as described in the previous section. The fitted force-displacement plot and the final results are shown in **Figure *D.1*** and **Table *D.1***, respectively.

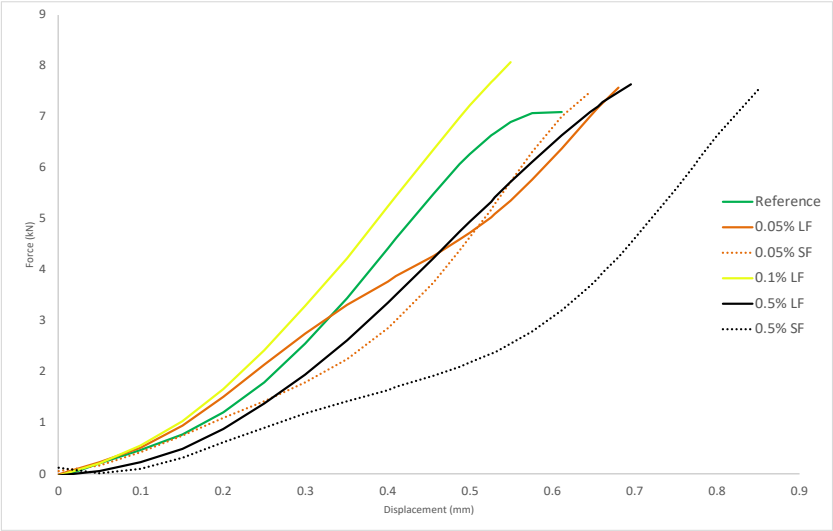

Figure D.1. Typical force-displacement curve after fitted in MATLAB

Table D.1. Final result of Semi-Circular Bending test (Strength, Energy, Toughness)

Fibre content	Strength	Average	K (Toughness)	Average	Strain	Average	Energy	Average
No fibre	4.314	3.989	25.692	23.758	0.70%	0.77%	0.025	0.025
	4.031		24.008		0.81%		0.029	
	4.050		24.124		0.88%		0.023	
	3.561		21.209		0.70%		0.022	
Fibre 0.05%	4.301	4.217	28.225	26.444	0.86%	0.84%	0.031	0.029
	4.104		24.446		0.88%		0.028	
	4.226		27.869		0.73%		0.028	
	4.237		25.236		0.87%		0.029	
Fibre 0.05% SH	*4.120*	*4.214*	*28.623*	*27.116*	*0.67%*	*0.85%*	*0.025*	*0.028*
	4.661		*27.764*		*1.33%*		*0.042*	
	4.259		*29.355*		*0.86%*		*0.028*	
	3.815		*22.724*		*0.55%*		*0.018*	
Fibre 0.1%	3.619	4.370	27.469	28.123	0.71%	0.76%	0.022	0.029
	4.755		28.323		0.86%		0.031	
	4.292		28.024		0.71%		0.032	
	4.815		28.677		0.77%		0.031	
Fibre 0.5%	4.372	4.465	30.782	29.027	0.86%	0.77%	0.031	0.032
	4.626		30.431		1.03%		0.043	
	4.639		29.747		0.65%		0.030	
	4.223		25.150		*0.55%*		0.023	
Fibre 0.5% SH	*4.484*	*4.346*	*26.709*	*27.662*	0.91%	*1.02%*	*0.035*	*0.030*
	4.575		*30.874*		*1.11%*		*0.031*	
	4.644		*31.132*		*1.20%*		*0.032*	
	3.682		*21.932*		*0.88%*		*0.023*	